

NIKHEF/95-070

ITP-SB-95-59

INLO-PUB-22/95

## Heavy quark coefficient functions at asymptotic values $Q^2 \gg m^2$

M. BUZA <sup>1</sup>*NIKHEF/UVA,**POB 41882, NL-1009 DB Amsterdam,  
The Netherlands.*

Y. MATIOUNINE AND J. SMITH

*Institute for Theoretical Physics,**State University of New York at Stony Brook,  
New York 11794-3840, USA.*R. MIGNERON <sup>2</sup>*Department of Applied Mathematics,  
University of Western Ontario,  
London, Ontario, N6A 5B9, Canada.*

W.L. VAN NEERVEN

*Instituut-Lorentz,**University of Leiden,**PO Box 9506, 2300 RA Leiden,  
The Netherlands.*

December 1995

### Abstract

In this paper we present the analytic form of the heavy-quark coefficient functions for deep-inelastic lepton-hadron scattering in the kinematical regime  $Q^2 \gg m^2$ . Here  $Q^2$  and  $m^2$  stand for the masses squared of the virtual photon and heavy quark respectively. The calculations have been performed up to next-to-leading order in the strong coupling constant  $\alpha_s$  using operator product expansion techniques. Apart from a check on earlier

---

<sup>1</sup>supported by the Foundation for Fundamental Research on Matter (FOM)

<sup>2</sup>partially supported by the Netherlands Organization for Scientific Research (NWO)

calculations, which however are only accessible via large computer programs, the asymptotic forms of the coefficient functions are useful for charm production at HERA when the condition  $Q^2 \gg m_c^2$  is satisfied. Furthermore the analytical expressions can also be used when one applies the variable heavy flavour scheme up to next-to-leading order in  $\alpha_s$ .

# 1 Introduction

The study of deep inelastic electroproduction has led to important information on the structure of the proton. This information is extracted from the structure functions  $F_2(x, Q^2)$  and  $F_L(x, Q^2)$  which appear in the cross section for deep inelastic lepton-hadron scattering. Here  $x$  denotes the Bjorken scaling variable and  $Q^2$  is the mass squared of the virtual photon exchanged between the lepton and the hadron. In the framework of perturbative Quantum Chromodynamics (QCD) these structure functions can be described by a convolution of parton densities with coefficient functions. The latter are calculable order by order in perturbation theory. However the parton densities cannot be computed yet since they are of a nonperturbative origin and have to be extracted from the data. Starting from the late sixties these densities have been obtained from many experiments. Until recently the analysis was carried out in the kinematical range  $0.01 < x < 0.95$  and  $Q^2 < 300$  (GeV/c)<sup>2</sup>. However since the advent of the HERA accelerator the kinematical region has been extended to much smaller values of  $x$  ( $x > 10^{-4}$ ) and much larger values of  $Q^2$  ( $Q^2 < 2 \times 10^4$  (GeV/c)<sup>2</sup>). The most recent results come from the H1 and ZEUS experiments at HERA, see [1] and [2] respectively.

The low- $x$  region is of great experimental as well as theoretical interest. The structure function  $F_2(x, Q^2)$  rises very steeply when  $x \rightarrow 0$  which can be mainly attributed to a corresponding increase in the gluon density. Therefore this density is a very important issue in the investigation of the small- $x$  structure of the proton. Since the gluon density appears together with the other parton densities in most cross sections, one has to look for those specific reactions in which it plays a dominant role so that it can be isolated from its partners. One of these processes is extrinsic charm production in deep inelastic electron-proton scattering. Here the dominant production mechanism is represented by the photon-gluon fusion process which is indeed the only one in the Born approximation. Next-to-leading order (NLO) calculations [3], to which also other processes contribute, reveal that this picture remains unaltered.

Apart from the interest in the gluon density, charm production also revived the important issue of how to treat the charm quark in deep inelastic scattering processes. Here one can distinguish between intrinsic [4] and extrinsic charm production. In the former case the charm is considered to be a part of the hadronic wave function and it is described by a parton density

in the hadron like the other light flavours ( $u, d, s$ ) and the gluon ( $g$ ). However this prescription is only correct if the charm quark can be treated as a massless particle which is certainly not the case at small- $Q^2$  values where threshold effects become important. In this region the charm quark has to be treated as a massive particle. On the other hand when  $Q^2 \gg m_c^2$ , where  $m_c$  is the charm mass, extrinsic charm production via the photon-gluon fusion process and its higher order QCD corrections reveal large logarithms of the type  $\alpha_s^k \ln^k(Q^2/m_c^2)$ . These large corrections bedevil the perturbation series and have therefore to be resummed via the renormalization group equations. This resummation entails the definition of a charm parton density in the hadron. Although a recent investigation [5] shows that the above logarithms lead to a rather stable cross section for charm production with respect to variations in the factorization and renormalization scale, the size of these large corrections warrants a special treatment. This is provided by the so-called variable flavour scheme (VFS) [6], [7]. In this scheme the treatment of the charm depends on the values chosen for  $Q^2$ . At low  $Q^2$ -values the deep inelastic structure functions are described by the light parton densities ( $u, d, s, g$ ). The charm contribution is given by the photon-gluon fusion process and its higher order QCD corrections. At large  $Q^2$  the charm is treated in the same way as the other light quarks and it is represented by a charm parton density in the hadron, which evolves in  $Q^2$ . In the intermediate  $Q^2$  region one has to make a smooth connection between the two different prescriptions. In [8], [9] and [10] this was done by adding and subtracting certain mass factorization terms. Notice that the above considerations also apply to bottom production when  $Q^2$  gets extremely large.

Up to now the VFS-scheme has only been applied to heavy flavour electroproduction using the Born approximation to the photon-gluon fusion process [8], [9] and [10]. It is our aim to extend this scheme to next-to-leading order in  $\alpha_s$ . For that purpose we will calculate the full two-loop operator matrix elements containing one heavy quark loop. This calculation provides us with the terms containing the logarithms  $\ln^k(\mu^2/m_c^2)$  which have to be subtracted from the charm cross section so that the final result becomes independent of the charm mass  $m_c$ . Here  $\mu$  denotes the operator renormalization scale which can be identified with the factorization scale. Using the two-loop operator matrix elements up to non-logarithmic terms and the NLO light parton coefficient functions in [11], we can construct an analytic form of the NLO heavy quark coefficient functions in the limit  $Q^2 \gg m_c^2$ . We will refer to these re-

sults as the asymptotic heavy quark coefficient functions. These expressions serve as a check on the exact calculation in [3] which is only available in a large computer program involving numerical integrations over several variables. Furthermore it enables us to see at which  $Q^2$ -values the asymptotic heavy quark coefficient functions coincide numerically with the exact ones, which gives an indication when the charm quark can be treated as a massless quark.

The content of this paper can be summarized as follows. In section 2 we introduce our notations and give an outline how the heavy quark coefficient functions can be determined in the asymptotic limit  $Q^2 \gg m_c^2$ . In section 3 we present the calculation of the full two-loop operator matrix element needed for the computation of the asymptotic form of the heavy quark coefficient function. The latter will be calculated in section 4. Finally in section 5 we will show at which  $Q^2$ -values the asymptotic form coincides with the exact one given in [3]. In Appendix A an exact analytic expression for the heavy quark coefficient function, which is valid for any  $Q^2$  and  $m_c^2$ , is presented in the case of the Compton subprocess. An important trick how to compute an operator matrix element with five different propagators is given in Appendix B. The long formulae obtained for the full operator matrix elements and the asymptotic heavy quark coefficient functions are presented in Appendices C and D respectively.

## 2 Heavy flavour coefficient functions

In the section we will show the connection between the heavy flavour coefficient functions computed in the asymptotic limit  $Q^2 \gg m^2$  and the operator matrix elements (OME's). Here  $Q^2$  denotes the mass squared of the virtual photon with momentum  $q$  ( $q^2 = -Q^2 < 0$ ) and  $m$  stands for the heavy flavour mass. The variable  $x$  is defined by  $x = Q^2/2p \cdot q$  (Bjorken scaling variable) where  $p$  stands for the momentum of the proton. The OME's arise when the local operators, which show up in the operator product expansion (OPE) of two electromagnetic currents, are sandwiched between the proton states indicated by  $|P \rangle$ . In the limit that  $x$  is fixed and  $Q^2 \gg M^2$ , where  $M$  denotes the mass of the proton, this OPE dominates the integrand of the hadronic structure tensor  $W_{\mu\nu}$ , which is defined by

$$W_{\mu\nu}(p, q) = \frac{1}{4\pi} \int d^4z e^{iq \cdot z} \langle P | [J_\mu(z), J_\nu(0)] | P \rangle . \quad (2.1)$$

This structure tensor arises when one computes the cross section for deep inelastic electroproduction of heavy flavours

$$e^-(\ell_1) + P(p) \rightarrow e^-(\ell_2) + Q(p_1)(\bar{Q}(p_2)) + 'X', \quad (2.2)$$

provided the above reaction is completely inclusive with respect to the hadronic state  $'X'$  as well as the heavy flavours  $Q(\bar{Q})$ . When the virtuality  $Q^2$  ( $q = \ell_1 - \ell_2$ ) of the exchanged photon is not too large ( $Q^2 \ll M_Z^2$ ) the reaction in (2.2) is dominated by the one-photon exchange mechanism and we can neglect any weak effects caused by the exchange of the Z-boson. In this case  $W_{\mu\nu}(p, q)$  in (2.1) can be written as

$$W_{\mu\nu}(p, q) = \frac{1}{2x} \left( g_{\mu\nu} - \frac{q_\mu q_\nu}{q^2} \right) F_L(x, Q^2) + \left( p_\mu p_\nu - \frac{p \cdot q}{q^2} (p_\mu q_\nu + p_\nu q_\mu) \right. \\ \left. + g_{\mu\nu} \frac{(p \cdot q)^2}{q^2} \right) \frac{F_2(x, Q^2)}{p \cdot q} . \quad (2.3)$$

The above formula follows from Lorentz covariance of  $W_{\mu\nu}(p, q)$ , parity invariance and the conservation of the electromagnetic current  $J_\mu$ . Besides the longitudinal structure function  $F_L(x, Q^2)$  and the structure function  $F_2(x, Q^2)$  one can also define the transverse structure function  $F_1(x, Q^2)$  which, however, depends on the two previous ones and is given by

$$F_1(x, Q^2) = \frac{1}{2x} [F_2(x, Q^2) - F_L(x, Q^2)] . \quad (2.4)$$

The above structure functions show up in the deep inelastic cross section of the process in (2.2) provided we integrate over the whole final state

$$\frac{d^2\sigma}{dx dy} = \frac{2\pi\alpha^2}{(Q^2)^2} S \left[ \{1 + (1 - y)^2\} F_2(x, Q^2) - y^2 F_L(x, Q^2) \right], \quad (2.5)$$

where  $S$  denotes the square of the c.m. energy of the electron proton system and the variables  $x$  and  $y$  are defined ( see above (2.1) ) as

$$x = \frac{Q^2}{2p \cdot q} \quad (0 < x \leq 1) \quad , \quad y = \frac{p \cdot q}{p \cdot \ell_1} \quad (0 < y < 1), \quad (2.6)$$

with

$$-q^2 = Q^2 = xyS . \quad (2.7)$$

In the QCD improved parton model the heavy flavour contribution to the hadronic structure functions can be expressed as integrals over the partonic scaling variable  $z = Q^2/(s + Q^2)$ , where  $s$  is the square of the photon-parton centre-of-mass energy ( $s \geq 4m^2$ ). This yields the following result

$$\begin{aligned} F_i(x, Q^2, m^2) = & x \int_x^{z_{max}} \frac{dz}{z} \left[ \frac{1}{n_f} \sum_{k=1}^{n_f} e_k^2 \left\{ \Sigma\left(\frac{x}{z}, \mu^2\right) L_{i,q}^S(z, Q^2, m^2, \mu^2) \right. \right. \\ & \left. \left. + G\left(\frac{x}{z}, \mu^2\right) L_{i,g}(z, Q^2, m^2, \mu^2) \right\} + \Delta\left(\frac{x}{z}, \mu^2\right) L_{i,q}^{NS}(z, Q^2, m^2, \mu^2) \right] \\ & + x e_H^2 \int_x^{z_{max}} \frac{dz}{z} \left\{ \Sigma\left(\frac{x}{z}, \mu^2\right) H_{i,q}(z, Q^2, m^2, \mu^2) \right. \\ & \left. + G\left(\frac{x}{z}, \mu^2\right) H_{i,g}(z, Q^2, m^2, \mu^2) \right\}, \quad (2.8) \end{aligned}$$

where  $i = 2, L$  and the upper boundary of the integration is given by  $z_{max} = Q^2/(4m^2 + Q^2)$ . The function  $G(z, \mu^2)$  stands for the gluon density. The singlet combination of the quark densities is defined by

$$\Sigma(z, \mu^2) = \sum_{i=1}^{n_f} \left( f_i(z, \mu^2) + \bar{f}_i(z, \mu^2) \right), \quad (2.9)$$

where  $f_i$  and  $\bar{f}_i$  stand for the light quark and anti-quark densities of species  $i$  respectively. The non-singlet combination of the quark densities is given by

$$\Delta(z, \mu^2) = \sum_{i=1}^{n_f} \left( e_i^2 - \frac{1}{n_f} \sum_{k=1}^{n_f} e_k^2 \right) \left( f_i(z, \mu^2) + \bar{f}_i(z, \mu^2) \right). \quad (2.10)$$

In the above expressions the charges of the light quark and the heavy quark are denoted by  $e_i$  and  $e_H$  respectively. Furthermore,  $n_f$  stands for the number of light quarks and  $\mu$  denotes the mass factorization scale, which we choose to be equal to the renormalization scale. The latter shows up in the running coupling constant defined by  $\alpha_s(\mu^2)$ . Like the parton densities the heavy quark coefficient functions  $L_{i,j}$  ( $i = 2, L$ ;  $j = q, g$ ) can also be divided into singlet and non-singlet parts which are indicated by the superscripts S and NS in eq. (2.8).

The distinction between the heavy quark coefficient functions  $L_{i,j}$  and  $H_{i,j}$  can be traced back to the different photon-parton production processes from which they originate. The functions  $L_{i,j}$  are attributed to the reactions where the virtual photon couples to the light quark, whereas  $H_{i,j}$  originates from the reactions where the virtual photon couples to the heavy quark. This explains why there is only a singlet part for  $H_{i,j}$  and that  $L_{i,j}$ ,  $H_{i,j}$  in eq. (2.8) are multiplied by  $e_i^2$ ,  $e_H^2$  respectively. In [3] the heavy quark coefficient functions have been calculated up to next-to-leading order(NLO). In the Born approximation (first order of  $\alpha_s$  or LO) one has the photon-gluon fusion process

$$\gamma^*(q) + g(k_1) \rightarrow Q(p_1) + \bar{Q}(p_2), \quad (2.11)$$

which leads to the lowest order contribution to  $H_{i,g}$  denoted by  $H_{i,g}^{(1)}$ . The next order is obtained by including the virtual gluon corrections to process (2.11) and the gluon bremsstrahlung process

$$\gamma^*(q) + g(k_1) \rightarrow g(k_2) + Q(p_1) + \bar{Q}(p_2), \quad (2.12)$$

both of which contribute to the second order term in  $H_{i,g}$  denoted by  $H_{i,g}^{(2)}$ . In addition to the above reaction we also have the subprocess where the gluon in (2.12) is replaced by a light (anti-) quark, i. e.

$$\gamma^*(q) + q(\bar{q})(k_1) \rightarrow q(\bar{q})(k_2) + Q(p_1) + \bar{Q}(p_2). \quad (2.13)$$

This process has however two different production mechanisms. The first one is given by the Bethe-Heitler process (see figs. 5a,b in [3]) and the second one can be attributed to the Compton reaction (see figs. 5c,d in [3]). In the case of the Bethe-Heitler process the virtual photon couples to the heavy quark and therefore this reaction contributes to  $H_{i,q}$ . This second order



contribution will be denoted by  $H_{i,q}^{(2)}$ . In the Compton reaction the virtual photon couples to the light (anti-) quark and its contribution to  $L_{i,q}^{\text{NS}}$  will be denoted by  $L_{i,q}^{\text{NS,(2)}}$ . Since  $L_{i,q}^{\text{S}}$  can be written as  $L_{i,q}^{\text{S}} = L_{i,q}^{\text{NS}} + L_{i,q}^{\text{PS}}$ ,  $L_{i,q}^{\text{NS,(2)}}$  also contributes to the singlet part of the coefficient function. In general the heavy quark coefficient functions are expanded in  $\alpha_s$  as follows

$$H_{i,g}(z, Q^2, m^2, \mu^2) = \sum_{k=1}^{\infty} \left(\frac{\alpha_s}{4\pi}\right)^k H_{i,g}^{(k)}(z, Q^2, m^2, \mu^2), \quad (2.14)$$

$$H_{i,q}(z, Q^2, m^2, \mu^2) = \sum_{k=2}^{\infty} \left(\frac{\alpha_s}{4\pi}\right)^k H_{i,q}^{(k)}(z, Q^2, m^2, \mu^2), \quad (2.15)$$

$$L_{i,j}^r(z, Q^2, m^2, \mu^2) = \sum_{k=2}^{\infty} \left(\frac{\alpha_s}{4\pi}\right)^k L_{i,j}^{r,(k)}(z, Q^2, m^2, \mu^2), \quad (2.16)$$

where  $r = \text{NS,S}$ . Finally we want to make the remark that there are no interference terms between the Bethe-Heitler and Compton reactions in (2.13) if one integrates over all final state momenta.

The complexity of the second order heavy quark coefficient functions prohibits publishing them in an analytic form, except for  $L_{i,q}^{\text{NS,(2)}}$ , which is given in Appendix A, so that they are only available in large computer programs [3], involving two-dimensional integrations. To shorten the long running time for these programs we have previously tabulated the coefficient functions in the form of a two dimensional array in the variables  $\eta$  and  $\xi$  in a different computer program [12]. These variables are defined by ( using  $s = (q + k_1)^2$ ,  $z = Q^2/(s + Q^2)$ , and  $\eta = (s - 4m^2)/(4m^2)$ )

$$\eta = \frac{(1-z)}{4z}\xi - 1 \quad , \quad \xi = \frac{Q^2}{m^2}. \quad (2.17)$$

This new program has shortened the computation of the charm structure functions  $F_i(x, Q^2, m_c^2)$  considerably as one only requires one integral over the variable  $z$  in (2.8), therefore making our results for the NLO corrections more amenable for phenomenological applications. However, when  $Q^2 \gg m^2$  it is possible to get complete analytic forms for the heavy quark coefficient functions which are similar to the ones presented for the light quark and

gluon coefficient functions given in [11]. To get the analytic form in the above asymptotic regime one can follow two approaches. The first one is to go back to the original calculation of the exact coefficient functions in [3] and repeat the computation of the Feynman graphs and the phase space integrals in the limit  $Q^2 \gg m^2$ . An example of such a calculation can be found in [13], where all photonic corrections to the initial state of the process  $e^- + e^+ \rightarrow \mu^- + \mu^+$  in the limit  $S \gg m_e^2$  were computed. However, this procedure is still quite complicated because one cannot neglect the fermion masses at too premature a stage which results in rather messy calculations. Fortunately, as one can find in [13], there exists an alternative method which we will use for the heavy quark coefficient functions.

In the limit  $Q^2 \gg m^2$  the heavy quark coefficient functions behave logarithmically as

$$H_{i,j}^{(k)}(z, Q^2, m^2, \mu^2) = \sum_{l=1}^k a_{i,j}^{(k,l)}\left(z, \frac{\mu^2}{m^2}\right) \ln^l \frac{Q^2}{m^2}, \quad (2.18)$$

with a similar expression for  $L_{i,j}^{(k)}$ . As has been already mentioned in the introduction these large logarithms  $\ln^l(Q^2/m^2)$  dominate the radiative corrections. This is in particular the case for charm production in the large  $Q^2$  region which is accessible to HERA experiments. The above large logarithms also arise when  $Q^2$  is kept fixed and  $m^2 \rightarrow 0$  so that they originate from collinear singularities. These collinear divergences can be removed via mass factorization. The latter proceeds in the following way. In the non-singlet case we have

$$C_{i,q}^{\text{NS}}\left(\frac{Q^2}{\mu^2}, n_f\right) + L_{i,q}^{\text{NS}}\left(\frac{Q^2}{m^2}, \frac{\mu^2}{m^2}\right) = \Gamma_{qq}^{\text{NS}}\left(\frac{\mu^2}{m^2}\right) \otimes C_{i,q}^{\text{NS}}\left(\frac{Q^2}{\mu^2}, n_f + 1\right). \quad (2.19)$$

For the singlet case the mass factorization becomes

$$C_{i,l}^{\text{S}}\left(\frac{Q^2}{\mu^2}, n_f\right) + L_{i,l}^{\text{S}}\left(\frac{Q^2}{m^2}, \frac{\mu^2}{m^2}\right) + H_{i,l}\left(\frac{Q^2}{m^2}, \frac{\mu^2}{m^2}\right) = \sum_k \Gamma_{kl}^{\text{S}}\left(\frac{\mu^2}{m^2}\right) \otimes C_{i,k}^{\text{S}}\left(\frac{Q^2}{\mu^2}, n_f + 1\right), \quad (2.20)$$

with  $k, l = q, g$ . Notice that in the above expression we have suppressed the  $z$ -dependence for simplicity. The convolution symbol is defined by

$$(f \otimes g)(z) = \int_0^1 dz_1 \int_0^1 dz_2 \delta(z - z_1 z_2) f(z_1) g(z_2). \quad (2.21)$$

The quantities  $\Gamma_{kl}$  and  $C_{i,k}$  ( $k, l = q, g$ ) which appear in the above equation stand for the transition functions and the light parton coefficient functions respectively. Notice that all mass dependence is transferred to the transition function  $\Gamma_{kl}$ . The removal of the logarithmic terms  $\ln^l(\mu^2/m^2)$  from the heavy flavour coefficient functions leads to an enhancement by one of the number of light flavours  $n_f$  in the light parton coefficient functions  $C_{i,k}$  - see eqs.(2.19), (2.20). The latter have been calculated up to second order in  $\alpha_s$  in [11]. Since these coefficient functions do not depend on the way one has regularized the collinear divergences in the parton cross sections (for a discussion see [14]) one can also use them in equations (2.19), (2.20). Now if one also knows the transition functions  $\Gamma_{kl}$  one can reconstruct the asymptotic behavior of the heavy flavour coefficient functions  $L_{i,k}$  and  $H_{i,k}$ . This is possible because the transition functions  $\Gamma_{kl}$  are identical to the operator matrix elements (OME) denoted by  $A_{kl}$ . The latter appear in the operator product expansion (OPE) of the commutator of the two electromagnetic currents in (2.1) near the lightcone. Suppressing the Lorentz index of the electromagnetic current the expansion can be written as

$$\lim_{z^2 \rightarrow 0} [J(z), J(0)] = \sum_k \sum_m C_k^{(m)}(z^2) z_{\mu_1} \cdots z_{\mu_m} O_k^{\mu_1 \cdots \mu_m}(0), \quad (2.22)$$

where the distributions  $C_k^{(m)}(z^2)$  ( $k = q, g$ ) are the Fourier transforms of the light parton coefficient functions  $C_k^{(m)}(Q^2/\mu^2)$  defined in (2.19), (2.20). Notice that the latter has been Mellin transformed according to

$$C_k^{(m)}\left(\frac{Q^2}{\mu^2}\right) = \int_0^1 dy y^{m-1} C_k\left(y, \frac{Q^2}{\mu^2}\right). \quad (2.23)$$

In the above expressions the index  $i$  ( $i = 2, L$ ) in  $C_{i,k}^{(m)}$  has been omitted since we suppressed the Lorentz index of the current  $J_\mu(z)$ . Inclusion of the latter index implies that one has two independent structure functions  $F_2$  and  $F_L$ . The quantity  $m$  refers to the spin of the local operators  $O_k^{\mu_1 \cdots \mu_m}$  which appear in the OPE (2.22). The latter are given by the non-singlet quark operator

$$O_{q,r}^{\mu_1 \cdots \mu_m}(x) = \frac{1}{2} i^{m-1} S \left[ \bar{\psi}(x) \gamma^{\mu_1} D^{\mu_2} \cdots D^{\mu_m} \frac{\lambda_r}{2} \psi(x) \right] + \text{trace terms}, \quad (2.24)$$

and the singlet operators

$$O_q^{\mu_1 \cdots \mu_m}(x) = \frac{1}{2} i^{m-1} S \left[ \bar{\psi}(x) \gamma^{\mu_1} D^{\mu_2} \cdots D^{\mu_m} \psi(x) \right] + \text{trace terms}, \quad (2.25)$$

$$O_g^{\mu_1 \dots \mu_m}(x) = \frac{1}{2} i^{m-2} S \left[ F_\alpha^{a, \mu_1}(x) D^{\mu_2} \dots D^{\mu_{m-1}} F^{a, \alpha \mu_m}(x) \right] + \text{trace terms} . \quad (2.26)$$

Here  $S$  denotes the symmetrization of the operators in their Lorentz indices  $\mu_i$  and the trace terms are needed to make them traceless. The  $\lambda_r$  in (2.24) represent the generators of the flavour algebra, whereas the index  $a$  in (2.26) is the colour index. The objects  $\psi(x)$ ,  $F_{\mu\nu}^a$  represent the quark field and the gluon field tensor respectively and  $D_\mu$  denotes the covariant derivative.

The OPE expansion in (2.22) can be applied in the limit  $Q^2 \gg m^2$  and fixed  $x$  so that the integrand in (2.1) gets its dominant contribution from the lightcone behavior of the current-current commutator. Inserting (2.22) in (2.1) and replacing the hadron state  $|P\rangle$  by a light quark or gluon one gets the relations

$$\tilde{\mathcal{F}}_{i,q}^{\text{NS}}\left(\frac{Q^2}{\mu^2}, \epsilon\right) + \tilde{L}_{i,q}^{\text{NS}}\left(\frac{Q^2}{m^2}, \frac{\mu^2}{m^2}, \epsilon\right) = \tilde{A}_{qq}^{\text{NS}}\left(\frac{\mu^2}{m^2}, \epsilon\right) \otimes C_{i,q}^{\text{NS}}\left(\frac{Q^2}{\mu^2}\right), \quad (2.27)$$

$$\begin{aligned} \tilde{\mathcal{F}}_{i,l}^{\text{S}}\left(\frac{Q^2}{\mu^2}, \epsilon\right) + \tilde{L}_{i,l}^{\text{S}}\left(\frac{Q^2}{m^2}, \frac{\mu^2}{m^2}, \epsilon\right) + \tilde{H}_{i,l}\left(\frac{Q^2}{m^2}, \frac{\mu^2}{m^2}, \epsilon\right) \\ = \tilde{A}_{kl}^{\text{S}}\left(\frac{\mu^2}{m^2}, \epsilon\right) \otimes C_{i,k}^{\text{S}}\left(\frac{Q^2}{\mu^2}\right), \end{aligned} \quad (2.28)$$

where  $i = 2, L$ ;  $k, l = q, g$ . Since the operators in (2.22) are already renormalized, the above expressions can be only collinearly divergent. The collinear divergences due to the presence of light partons are regularized by the method of  $n$ -dimensional regularization. They are indicated by the pole terms  $(1/\epsilon)^i$  ( $\epsilon = n - 4$ ). However the collinear divergences due to the heavy quarks are regularized by the mass  $m$  which shows up in the form of logarithms of the type  $\ln^i(Q^2/m^2)$ ,  $\ln^i(\mu^2/m^2)$ . The objects  $\tilde{\mathcal{F}}_{i,k}$  denote the light parton structure functions. The OME's  $\tilde{A}_{kl}$  are defined by

$$\tilde{A}_{kl}\left(\frac{\mu^2}{m^2}, \epsilon\right) = \langle l | O_k | l \rangle, \quad (2.29)$$

where  $|l\rangle$  is a light quark or a gluon state and all quantities depending on the pole terms are indicated by a tilde. If the latter are removed via

mass factorization one obtains expressions (2.19), (2.20) which implies the following identification

$$\Gamma_{qq}^{\text{NS}}\left(\frac{\mu^2}{m^2}\right) = A_{qq}^{\text{NS}}\left(\frac{\mu^2}{m^2}\right), \quad (2.30)$$

$$\Gamma_{kl}^{\text{S}}\left(\frac{\mu^2}{m^2}\right) = A_{kl}^{\text{S}}\left(\frac{\mu^2}{m^2}\right). \quad (2.31)$$

For the computation of the asymptotic behaviour of the heavy quark coefficient functions corresponding to the processes (2.11)-(2.13) one needs the following quantities. For processes (2.11) and (2.12) we have to calculate the one-loop OME  $A_{Qg}^{(1)}$  and the two-loop OME  $A_{Qg}^{(2)}$  respectively. They are represented by the Feynman graphs in fig.1 and fig.2. The Bethe-Heitler process given by reaction (2.13) corresponds to the two-loop OME  $A_{Qq}^{\text{PS},(2)}$  in fig.3 whereas the Compton process (2.13) is related to  $A_{qq}^{\text{NS},(2)}$  with the two-loop OME's in fig.4. The calculation of the graphs in figs. 1-4 and the derivation of the asymptotic form of the heavy quark coefficient functions will be the aim of the next two sections.

### 3 Calculation of the two-loop operator matrix elements

Before presenting the results of our calculation of the OME's we will first derive the general structure of the OME's discussed in the last section. If we insert the OPE (2.22) into the structure tensor  $W_{\mu\nu}$  in (2.1) the OME's which are derived from the Feynman graphs in figs.1-4 will be computed in the forward direction. The latter means that the momentum leaving the operator vertex equals zero. Further if one puts the momentum, indicated by  $p$ , of the external light quark and gluon off-shell ( $p^2 < 0$ ) only ultraviolet (UV) singularities appear in the OME's. Using this off-mass-shell assignment one can express the renormalized as well as the unrenormalized OME's into the renormalization group coefficients as is done in [15]. However for our computations we have to put the external momentum on-shell ( $p^2 = 0$ ) so that the OME's turn into genuine S-matrix elements. This mass assignment implies that in addition to UV divergences one also encounters collinear (C) divergences which originate from the coupling of the external on-shell massless quanta to internal massless quanta. In the computation of the Feynman graphs both types of divergences will be regularized using the technique of  $n$ -dimensional regularization. However since both singularities in the OME's will manifest themselves in the form of pole terms of the type  $\epsilon^{-k}$  ( $\epsilon = n - 4$ ) it is very hard to trace back their origins. Nevertheless one can express the OME's into the renormalization group coefficients in a similar way as has been derived for the off-shell case in [15]. Where possible we will make a distinction between UV-pole terms and C-pole terms, which are indicated by  $\epsilon_{UV}^{-k}$  and  $\epsilon_C^{-k}$  respectively, and identify them  $\epsilon_{UV} = \epsilon_C$  when it is appropriate.

In the subsequent part of this section we will construct the OME's, corresponding to the graphs in figs.1-4, in such a way that the coefficients of the pole terms are given by the renormalization group. These coefficients are products of the terms appearing in the beta-function and the AP-splitting functions (anomalous dimensions) [16]. The purpose of this presentation is threefold. First we need these coefficients for the construction of the heavy quark coefficient functions in the next section. Second since the renormalization group coefficients are known in the literature we can predict the residues of the pole terms so that these expressions serve as a check on our calculations. Third it is much easier to show the renormalization and mass factor-

ization for the algebraic expressions, which are short, than for the analytic formulae in our calculations because the latter are rather long.

The OME's  $A_{ij}$  can be expanded in a perturbation series as follows

$$A_{ij} = \sum_{k=0}^{\infty} \left(\frac{\alpha_s}{4\pi}\right)^k A_{ij}^{(k)}. \quad (3.1)$$

In the following discussion we distinguish three different types of OME's. First we have the unrenormalized ones indicated by  $\hat{A}_{ij}$ . They contain UV- as well as C-singularities. Second after renormalization the UV-divergences are removed and we are left by the OME's defined by  $\tilde{A}_{ij}$  which still contain C-divergences. The latter have to be removed via mass factorization so that the  $\tilde{A}_{ij}$  turn into the finite OME's indicated by  $A_{ij}$ . Notice that the expansion in (3.1) holds for all three different types of OME's.

The renormalization of  $\hat{A}_{ij}$  proceeds in three steps. First we will perform mass renormalization for which we choose the on-mass-shell scheme. This implies that the bare mass  $\hat{m}$ , which occurs in  $\hat{A}_{ij}$  has to be replaced by

$$\hat{m} = m\left(1 + \frac{\hat{\alpha}_s}{4\pi}\delta m\right) \quad , \quad \delta m = C_F S_\epsilon \left(\frac{m^2}{\mu^2}\right)^{\epsilon/2} \left\{ \frac{6}{\epsilon_{\text{UV}}} - 4 \right\}, \quad (3.2)$$

so that the mass renormalized  $\hat{A}_{ij}$  reads up to order  $\alpha_s^2$

$$\hat{A}_{ij} = \hat{A}_{ij}^{(0)} + \left(\frac{\hat{\alpha}_s}{4\pi}\right)\hat{A}_{ij}^{(1)} + \left(\frac{\hat{\alpha}_s}{4\pi}\right)^2 \left\{ \hat{A}_{ij}^{(2)} + \delta m \frac{d}{dm} \hat{A}_{ij}^{(1)} \right\}. \quad (3.3)$$

Notice that the zeroth order term  $\hat{A}_{ij}^{(0)} = \delta_{ij}$  is mass independent. In the above perturbation series the quantities  $\mu^2$  and  $S_\epsilon$  are artefacts of  $n$ -dimensional regularization. The mass parameter  $\mu$  originates from the dimensionality of the gauge coupling constant  $g$  ( $\alpha_s = g^2/4\pi$ ) in  $n$ -dimensions and should not be confused with the renormalization and mass-factorization scale. However if one only subtracts the pole-terms like in the  $\overline{\text{MS}}$ -scheme the mass parameter  $\mu$  turns into the afore-mentioned scales. The spherical factor  $S_\epsilon$  is defined as

$$S_\epsilon = \exp \left\{ \frac{\epsilon}{2} (\gamma_E - \ln 4\pi) \right\}, \quad (3.4)$$

and the colour factor is

$$C_F = \frac{N^2 - 1}{2N}, \quad (3.5)$$

in SU(N). Further  $\hat{\alpha}_s$  denotes the bare coupling constant which will be renormalized as follows

$$\hat{\alpha}_s = \alpha_s(\mu^2) \left( 1 + \frac{\alpha_s(\mu^2)}{4\pi} \delta\alpha_s \right), \quad (3.6)$$

$$\delta\alpha_s = S_\epsilon \left\{ \frac{2\beta_0}{\epsilon_{UV}} + \frac{2\beta_{0,H}}{\epsilon_{UV}} \left( \frac{m_H^2}{\mu^2} \right)^{\epsilon/2} \left( 1 + \frac{1}{8} \zeta(2) \epsilon_{UV}^2 \right) \right\}. \quad (3.7)$$

Here a summation over the heavy quarks  $H$  ( $H = c, b, t$ ) is understood and  $\zeta(2) = \pi^2/6$  is the Riemann zeta-function. Further  $\beta_0$  is the lowest order term in the series expansion of the beta-function, which up to two-loop order, is given by

$$\beta(g) = -\beta_0 \frac{g^3}{16\pi^2} - \beta_1 \frac{g^5}{(16\pi^2)^2}, \quad (3.8)$$

where

$$\beta_0 = \frac{11}{3} C_A - \frac{4}{3} T_f n_f,$$

and

$$\beta_1 = \frac{34}{3} C_A^2 - 4 C_F T_f n_f - \frac{20}{3} C_A T_f n_f.$$

Here  $C_A$  and  $T_f$  denote colour factors of SU(N)

$$C_A = N \quad , \quad T_f = \frac{1}{2}, \quad (3.9)$$

and  $n_f$  denotes the number of light flavours which enter via the fermion-loop contributions to the gluon self-energy. However besides the light quarks also the heavy quarks with mass  $m_H$  contribute to the renormalized coupling constant  $\alpha_s$ . This contribution is indicated in (3.7) by  $\beta_{0,H} = -4T_f/3$  and  $m_H \geq m$ . The coupling constant renormalization in (3.6), (3.7) is determined in the  $\overline{\text{MS}}$ -scheme as far as the light flavours and the gluon are concerned. In addition we make the choice that the heavy quarks decouple in the running strong coupling constant  $\alpha_s(\mu^2)$  for  $\mu^2 < m_H^2$  and the renormalized OME's. The factor  $1 + \epsilon^2 \zeta(2)/8$  in (3.7) arises from the requirement that  $\Pi_H(0, m_H^2) =$



0, where  $\Pi_H(p^2, m_H^2)$  is the contribution to the gluon self-energy due to the heavy quark loops indicated by  $H$ . After coupling constant renormalization  $\hat{A}_{ij}$  takes the form up to  $O(\alpha_s^2)$

$$\hat{A}_{ij} = \delta_{ij} + \left(\frac{\alpha_s}{4\pi}\right)\hat{A}_{ij}^{(1)} + \left(\frac{\alpha_s}{4\pi}\right)^2\left\{\hat{A}_{ij}^{(2)} + \delta m \frac{d}{dm}\hat{A}_{ij}^{(1)} + \delta\alpha_s\hat{A}_{ij}^{(1)}\right\}. \quad (3.10)$$

The remaining UV-divergences are removed by operator renormalization which is achieved by

$$\hat{A}_{ij}\left(\epsilon_{\text{UV}}, \epsilon_{\text{C}}, \frac{\mu^2}{m^2}, \alpha_s\right) = Z_{ik}(\epsilon_{\text{UV}}, \alpha_s) \otimes \tilde{A}_{kj}\left(\epsilon_{\text{C}}, \frac{\mu^2}{m^2}, \alpha_s\right), \quad (3.11)$$

where  $Z_{ij}$  ( $i, j = q, g$ ) are the operator renormalization constants corresponding to the operators in (2.24)-(2.26). Notice that for the non-singlet operator in (2.24)  $Z_{qq}^{\text{NS}}$  is a real number, whereas for the singlet operators in (2.25), (2.26)  $Z_{ij}$  becomes a matrix. The operator matrix elements can be expanded in  $\alpha_s$  analogous to  $A_{ij}$  in (3.1) as follows

$$Z_{ij} = \sum_{k=0}^{\infty} \left(\frac{\alpha_s}{4\pi}\right)^k Z_{ij}^{(k)}, \quad (3.12)$$

so that the renormalized OME's  $\tilde{A}_{ij}$  in (3.11) read up to  $O(\alpha_s^2)$ , (using  $Z_{ij}^{(0)} = \delta_{ij}$ )

$$\begin{aligned} \tilde{A}_{ij} = & \delta_{ij} + \left(\frac{\alpha_s}{4\pi}\right)[\hat{A}_{ij}^{(1)} + Z_{ij}^{-1,(1)}] + \left(\frac{\alpha_s}{4\pi}\right)^2\left\{\hat{A}_{ij}^{(2)} + \delta m \frac{d}{dm}\hat{A}_{ij}^{(1)} \right. \\ & \left. + \delta\alpha_s\hat{A}_{ij}^{(1)} + Z_{ik}^{-1,(1)}\hat{A}_{kj}^{(1)} + Z_{ij}^{-1,(2)}\right\}, \end{aligned} \quad (3.13)$$

where  $Z_{ij}^{-1,(k)}$  are the expansion coefficients of the inverse matrix  $Z^{-1}$ . Choosing the  $\overline{\text{MS}}$ -scheme one obtains the following expression (see [15]) up to  $O(\alpha_s^2)$

$$\begin{aligned} Z_{ij}(\epsilon_{\text{UV}}, \alpha_s) = & \delta_{ij} + \left(\frac{\alpha_s}{4\pi}\right)S_\epsilon\left[-\frac{1}{\epsilon_{\text{UV}}}P_{ij}^{(0)}\right] \\ & + \left(\frac{\alpha_s}{4\pi}\right)^2 S_\epsilon^2\left[\frac{1}{\epsilon_{\text{UV}}^2}\left\{\frac{1}{2}P_{ik}^{(0)} \otimes P_{kj}^{(0)} + (\beta_0 + \beta_{0,H})P_{ij}^{(0)}\right\}\right. \\ & \left. - \frac{1}{\epsilon_{\text{UV}}}\delta\alpha_s P_{ij}^{(0)} - \frac{1}{2\epsilon_{\text{UV}}}P_{ij}^{(1)}\right]. \end{aligned} \quad (3.14)$$

Here  $P_{ij}^{(0)}$  and  $P_{ij}^{(1)}$  stand for the first and second order AP-splitting functions [16] respectively which have been calculated in the literature (see [16], [17], [18], [19], [20]). Notice that in our notation  $A_{ij}$  and  $Z_{ij}$  depend on the partonic Bjorken scaling variable  $z$  in (2.8) which for convenience has been suppressed in our formulae. Hence instead of multiplications we have to deal with convolutions denoted by the symbol  $\otimes$ , which is defined in (2.21). Furthermore the AP-splitting functions are related to the anomalous dimensions  $\gamma_{ij}^{(m)}$  of the composite operators in (2.24)-(2.26) via the Mellin transform

$$\gamma_{ij}^{(m),(k)} = - \int_0^1 dz z^{m-1} P_{ij}^{(k)}(z). \quad (3.15)$$

Finally we have to remove the  $C$ -divergences appearing in  $\tilde{A}_{ij}$  (3.11). This is achieved by performing mass factorization which proceeds as

$$\tilde{A}_{ij}(\epsilon_C, \frac{\mu^2}{m^2}, \alpha_s) = A_{ik}(\frac{\mu^2}{m^2}, \alpha_s) \otimes \Gamma_{kj}(\epsilon_C, \alpha_s), \quad (3.16)$$

where  $A_{ij}$  denote the finite OME's which do not have UV or C divergences anymore. The quantities  $\Gamma_{ij}$  stand for the transition functions which have the same properties as  $Z_{ij}$  mentioned above (3.12). Like  $A_{ij}$  and  $Z_{ij}$  the  $\Gamma_{ij}$  can be expanded as a power series in  $\alpha_s$

$$\Gamma_{ij} = \sum_{k=0}^{\infty} \left(\frac{\alpha_s}{4\pi}\right)^k \Gamma_{ij}^{(k)}, \quad (3.17)$$

so that the mass factorized OME's  $A_{ij}$  read up to  $O(\alpha_s^2)$  (using  $\Gamma_{ij}^{(0)} = \delta_{ij}$ )

$$\begin{aligned} A_{ij} &= \delta_{ij} + \left(\frac{\alpha_s}{4\pi}\right) [\hat{A}_{ij}^{(1)} + Z_{ij}^{-1,(1)} + \Gamma_{ij}^{-1,(1)}] \\ &+ \left(\frac{\alpha_s}{4\pi}\right)^2 \left[ \hat{A}_{ij}^{(2)} + \delta m \frac{d}{dm} \hat{A}_{ij}^{(1)} + \delta \alpha_s \hat{A}_{ij}^{(1)} + Z_{ik}^{-1,(1)} \hat{A}_{kj}^{(1)} + Z_{ij}^{-1,(2)} \right. \\ &\left. + \left\{ \hat{A}_{ik}^{(1)} + Z_{ik}^{-1,(1)} \right\} \otimes \Gamma_{kj}^{-1,(1)} + \Gamma_{ij}^{-1,(2)} \right], \end{aligned} \quad (3.18)$$

where  $\Gamma_{ij}^{-1,(k)}$  are the expansion coefficients of the inverse matrix  $\Gamma^{-1}$ . Choosing the  $\overline{\text{MS}}$ -scheme one obtains the following expression (see [11]) up to  $O(\alpha_s^2)$

$$\Gamma_{ij}(\epsilon_C, \alpha_s) = \delta_{ij} + \left(\frac{\alpha_s}{4\pi}\right) S_{\epsilon} \left[ \frac{1}{\epsilon_C} P_{ij}^{(0)} \right]$$

$$+ \left(\frac{\alpha_s}{4\pi}\right)^2 S_\epsilon^2 \left[ \frac{1}{\epsilon_C^2} \left\{ \frac{1}{2} P_{ik}^{(0)} \otimes P_{kj}^{(0)} + \beta_0 P_{ij}^{(0)} \right\} + \frac{1}{2\epsilon_C} P_{ij}^{(1)} \right]. \quad (3.19)$$

If all quarks would be massless we would have the identity  $\Gamma_{ij} = Z_{ij}^{-1}$ . However since the heavy quark  $Q$  is massive it does not contribute to those splitting functions  $P_{ij}^{(k)}$  which appear in the transition functions. Hence in this case  $i$  and  $j$  only represent the light quarks and the gluon. This is in contrast to the operator renormalization constant  $Z_{ij}$  where  $i$  and  $j$  can also stand for the heavy quark. The same assertion holds for the heavy flavour contributions to the beta-function given by  $\beta_{0,H}$  ( $m_H^2 \geq Q^2$ ) which shows up in (3.14) but not in (3.19). The reason is that the mass  $m$  of the heavy quark acts as a regulator for the C-divergences but not for the UV-singularities.

Using the master formula in (3.18) one can now construct the general form of the finite OME  $A_{ij}$  as well as the unrenormalized OME  $\hat{A}_{ij}$  expressed in their renormalization group coefficients  $\beta_0$ ,  $\beta_{0,H}$  and  $P_{ij}^{(k)}$  ( $k = 0, 1$ ;  $i, j = q, g$ ). For convenience we will take for  $\hat{A}_{ij}$  the representation (3.3), where the mass renormalization has been already carried out.

Starting with the one-loop OME  $\hat{A}_{Qg}^{(1)}$ , which receives contributions from the graphs in fig.1, we obtain

$$\hat{A}_{Qg}^{(1)} = S_\epsilon \left(\frac{m^2}{\mu^2}\right)^{\epsilon/2} \left\{ -\frac{1}{\epsilon_{UV}} P_{qg}^{(0)} + a_{Qg}^{(1)} + \epsilon_{UV} \bar{a}_{Qg}^{(1)} \right\}. \quad (3.20)$$

The renormalization group coefficients are given by

$$\begin{aligned} P_{qg}^{(0)} &= 8T_f [z^2 + (1-z)^2], \\ a_{Qg}^{(1)} &= 0, \\ \bar{a}_{Qg}^{(1)} &= -\frac{1}{8} \zeta(2) P_{qg}^{(0)}. \end{aligned} \quad (3.21)$$

The expression for the two-loop contribution to  $\hat{A}_{Qg}$  (see fig.2) can be written as

$$\hat{A}_{Qg}^{(2)} = S_\epsilon^2 \left(\frac{m^2}{\mu^2}\right)^\epsilon \left[ \frac{1}{\epsilon^2} \left\{ \frac{1}{2} P_{qg}^{(0)} \otimes (P_{qq}^{(0)} - P_{gg}^{(0)}) + \beta_0 P_{qg}^{(0)} \right\} \right]$$

$$\begin{aligned}
& +\frac{1}{\epsilon}\left\{-\frac{1}{2}P_{qg}^{(1)}-2\beta_0a_{Qg}^{(1)}-a_{Qg}^{(1)}\otimes(P_{qq}^{(0)}-P_{gg}^{(0)})\right\}+a_{Qg}^{(2)}] \\
& -\frac{2}{\epsilon}S_\epsilon\beta_{0,H}\left(\frac{m_H^2}{\mu^2}\right)^{\epsilon/2}\left(1+\frac{\epsilon^2}{8}\zeta(2)\right)\hat{A}_{Qg}^{(1)}. \tag{3.22}
\end{aligned}$$

Notice that in the above expression the pole terms  $\epsilon^{-k}$  stand for the UV as well as C-divergences so that we have put  $\epsilon_{UV} = \epsilon_C$ . Further we infer from the literature that

$$\begin{aligned}
P_{qq}^{(0)} &= 4C_F\left[2\left(\frac{1}{1-z}\right)_+ - 1 - z + \frac{3}{2}\delta(1-z)\right], \\
P_{gg}^{(0)} &= 8C_A\left[\left(\frac{1}{1-z}\right)_+ + \frac{1}{z} - 2 + z - z^2\right] + 2\beta_0\delta(1-z), \\
P_{qg}^{(1)} &= 8C_FT_f\left[2(1-2z+2z^2)\{\ln^2(1-z) - 2\ln z \ln(1-z) - 2\zeta(2)\}\right. \\
&\quad + (1-2z+4z^2)\ln^2 z + 8z(1-z)\ln(1-z) + (3-4z+8z^2)\ln z \\
&\quad \left.+ 14 - 29z + 20z^2\right] \\
&\quad + 8C_AT_f\left[(1+2z+2z^2)\{\ln^2 z - 4\ln z \ln(1+z) - 4\text{Li}_2(-z) - 2\zeta(2)\}\right. \\
&\quad \left.+ 2(1-2z+2z^2)[\zeta(2) - \ln^2(1-z)] - (3+6z+2z^2)\ln^2 z\right. \\
&\quad \left.- 8z(1-z)\ln(1-z) + \left(2+16z+\frac{88}{3}z^2\right)\ln z\right. \\
&\quad \left.+ \frac{2}{9}\left(\frac{20}{z} - 18 + 225z - 218z^2\right)\right], \tag{3.23}
\end{aligned}$$

and  $a_{Qg}^{(2)}$  (3.22) has to be computed in this paper. In the above and subsequent expressions the functions  $\text{Li}_n(z)$  denote the polylogarithms which can be found in [21]. The finite OME's follow from (3.18) where we have

$$\begin{aligned}
A_{Qg}^{(1)} &= \hat{A}_{Qg}^{(1)} + Z_{qg}^{-1,(1)} \\
&= -\frac{1}{2}P_{qg}^{(0)}\ln\frac{m^2}{\mu^2} + a_{Qg}^{(1)}, \tag{3.24}
\end{aligned}$$

and

$$\begin{aligned}
A_{Qg}^{(2)} &= \hat{A}_{Qg}^{(2)} + \delta\alpha_s \hat{A}_{Qg}^{(1)} + Z_{qq}^{-1,(1)} \otimes \hat{A}_{Qg}^{(1)} + Z_{gg}^{-1,(1)} \otimes \hat{A}_{gg}^{(1)} \\
&\quad + Z_{gg}^{-1,(2)} + (\hat{A}_{Qg}^{(1)} + Z_{qq}^{-1,(1)}) \otimes \Gamma_{gg}^{-1,(1)} \\
&= \left\{ \frac{1}{8} P_{qg}^{(0)} \otimes P_{qg}^{(0)} - \frac{1}{8} P_{qg}^{(0)} \otimes P_{gg}^{(0)} + \frac{1}{4} \beta_0 P_{qg}^{(0)} \right\} \ln^2 \frac{m^2}{\mu^2} \\
&\quad + \left\{ -\frac{1}{2} P_{qg}^{(1)} - \beta_0 a_{Qg}^{(1)} - \frac{1}{2} P_{qq}^{(0)} \otimes a_{Qg}^{(1)} + \frac{1}{2} P_{gg}^{(0)} \otimes a_{Qg}^{(1)} \right\} \ln \frac{m^2}{\mu^2} \\
&\quad + a_{Qg}^{(2)} + 2\beta_0 \bar{a}_{Qg}^{(1)} + P_{qq}^{(0)} \otimes \bar{a}_{Qg}^{(1)} - P_{gg}^{(0)} \otimes \bar{a}_{Qg}^{(1)}. \tag{3.25}
\end{aligned}$$

In eqs.(3.24), (3.25) we have used the heavy flavour contributions ( $m_H^2 \geq Q^2$ ) to the one loop OME  $A_{gg}^{(1)}$  in fig.1c which is given by

$$A_{gg}^{(1)} = S_\epsilon \left( \frac{m_H^2}{\mu^2} \right)^{\epsilon/2} \left[ -\frac{2}{\epsilon_{\text{UV}}} \beta_{0,H} - \frac{1}{4} \epsilon_{\text{UV}} \beta_{0,H} \zeta(2) \right], \tag{3.26}$$

and the constants

$$\begin{aligned}
Z_{qg}^{-1,(1)} &= S_\epsilon \left[ \frac{1}{\epsilon_{\text{UV}}} P_{qg}^{(0)} \right], \\
Z_{qg}^{-1,(2)} &= S_\epsilon^2 \left[ \frac{1}{\epsilon_{\text{UV}}^2} \left\{ \frac{1}{2} P_{qg}^{(0)} \otimes (P_{qq}^{(0)} + P_{gg}^{(0)}) - \beta_0 P_{qg}^{(0)} \right\} \right. \\
&\quad \left. + \frac{1}{\epsilon_{\text{UV}}} \delta\alpha_s P_{qg}^{(0)} + \frac{1}{2\epsilon_{\text{UV}}} P_{qg}^{(1)} \right], \\
Z_{qq}^{-1,(1)} &= S_\epsilon \left[ \frac{1}{\epsilon_{\text{UV}}} P_{qq}^{(0)} \right], \\
\Gamma_{gg}^{-1,(1)} &= S_\epsilon \left[ -\frac{1}{\epsilon_{\text{C}}} P_{gg}^{(0)} \right]. \tag{3.27}
\end{aligned}$$

Notice that due to our scheme for  $\alpha_s$  in (3.7)  $\beta_{0,H}$  and  $m_H$  ( $m_H^2 \geq Q^2$ ) have completely disappeared from  $A_{Qg}^{(2)}$  (3.25).

The renormalization and the mass factorization of the OME's  $\hat{A}_{Qq}^{\text{PS},(2)}$  in fig.3 proceeds in the same way as done for  $\hat{A}_{Qg}$ . The superscript PS stands for 'pure singlet' and it originates from the definition that the singlet OME  $A_{qq}^{\text{S}}$  can be decomposed into

$$A_{qq}^{\text{S}} = A_{qq}^{\text{NS}} + A_{qq}^{\text{PS}}, \quad (3.28)$$

where  $A_{qq}^{\text{NS}}$  stands for the non-singlet OME. The unrenormalized OME reads

$$\begin{aligned} \hat{A}_{Qq}^{\text{PS},(2)} = S_\epsilon^2 \left( \frac{m^2}{\mu^2} \right)^\epsilon & \left[ \frac{1}{\epsilon^2} \left\{ -\frac{1}{2} P_{qg}^{(0)} \otimes P_{gq}^{(0)} \right\} + \frac{1}{\epsilon} \left\{ -\frac{1}{2} P_{qq}^{\text{PS},(1)} \right. \right. \\ & \left. \left. + a_{Qg}^{(1)} \otimes P_{gq}^{(0)} \right\} + a_{Qq}^{\text{PS},(2)} \right]. \end{aligned} \quad (3.29)$$

Like in the case of  $\hat{A}_{Qg}^{(2)}$  we did not make any distinction between UV and C-singular pole terms  $\epsilon^{-k}$  ( $\epsilon_{\text{UV}} = \epsilon_{\text{C}}$ ). The renormalization group coefficients are given by (see also (3.21))

$$\begin{aligned} P_{gq}^{(0)} &= 4C_F \left[ \frac{2}{z} - 2 + z \right], \\ P_{qq}^{\text{PS},(1)} &= 8C_F T_f \left[ -2(1+z) \ln^2 z + \left( 2 + 10z + \frac{16}{3} z^2 \right) \ln z \right. \\ & \left. + \frac{40}{9z} - 4 + 12z - \frac{112}{9} z^2 \right], \end{aligned} \quad (3.30)$$

and  $a_{Qq}^{\text{PS},(2)}$  will be calculated in this paper. The finite OME  $A_{Qq}^{\text{PS},(2)}$  can be again derived from (3.18) which yields

$$\begin{aligned} A_{Qq}^{\text{PS},(2)} &= \hat{A}_{Qq}^{\text{PS},(2)} + \left( Z_{qq}^{\text{PS}} \right)^{-1,(2)} + \left( \hat{A}_{Qg}^{(1)} + Z_{qg}^{-1,(1)} \right) \otimes \Gamma_{gq}^{-1,(1)} \\ &= \left\{ -\frac{1}{8} P_{qg}^{(0)} \otimes P_{gq}^{(0)} \right\} \ln^2 \frac{m^2}{\mu^2} \\ &+ \left\{ -\frac{1}{2} P_{qq}^{\text{PS},(1)} + \frac{1}{2} a_{Qg}^{(1)} \otimes P_{gq}^{(0)} \right\} \ln \frac{m^2}{\mu^2} \\ &+ a_{Qq}^{\text{PS},(2)} - \bar{a}_{Qg}^{(1)} \otimes P_{gq}^{(0)}. \end{aligned} \quad (3.31)$$

Here we have used the renormalization group constants (see also (3.21),(3.30))

$$\begin{aligned} (Z_{qq}^{\text{PS}})^{-1,(2)} &= S_\epsilon^2 \left[ \frac{1}{\epsilon_{\text{UV}}^2} \left\{ \frac{1}{2} P_{qq}^{(0)} \otimes P_{qq}^{(0)} \right\} + \frac{1}{2\epsilon_{\text{UV}}} P_{qq}^{\text{PS},(1)} \right], \\ \Gamma_{qq}^{-1,(1)} &= S_\epsilon \left[ -\frac{1}{\epsilon_{\text{C}}} P_{qq}^{(0)} \right]. \end{aligned} \quad (3.32)$$

The last OME which we have to deal with is represented by the heavy quark loop contribution to  $A_{qq}^{\text{NS},(2)}$  in fig.4. The unrenormalized expression reads

$$\hat{A}_{qq,Q}^{\text{NS},(2)} = S_\epsilon^2 \left( \frac{m^2}{\mu^2} \right)^\epsilon \left[ \frac{1}{\epsilon_{\text{UV}}^2} \left\{ -\beta_{0,Q} P_{qq}^{(0)} \right\} + \frac{1}{\epsilon_{\text{UV}}} \left\{ -\frac{1}{2} P_{qq,Q}^{\text{NS},(1)} \right\} + a_{qq,Q}^{\text{NS},(2)} \right]. \quad (3.33)$$

Contrary to  $\hat{A}_{Qg}^{(2)}$  and  $A_{Qq}^{\text{PS},(2)}$  the above OME only contains UV-divergences since the heavy quark  $Q$  prevents  $\hat{A}_{qq,Q}^{\text{NS},(2)}$  to be C-singular provided we choose the coupling constant renormalization scheme in (3.7). The renormalization group coefficients in (3.33) are given by

$$\begin{aligned} \beta_{0,Q} &= -\frac{4}{3} T_f, \\ P_{qq,Q}^{\text{NS},(1)} &= C_F T_f \left[ -\frac{160}{9} \left( \frac{1}{1-z} \right)_+ + \frac{176}{9} z - \frac{16}{9} - \frac{16}{3} \frac{1+z^2}{1-z} \ln z \right. \\ &\quad \left. + \delta(1-z) \left( -\frac{4}{3} - \frac{32}{3} \zeta(2) \right) \right]. \end{aligned} \quad (3.34)$$

Since  $\hat{A}_{qq,Q}^{\text{NS},(2)}$  does not contain C-divergences we only need operator renormalization to render it finite. From (3.18) we infer

$$\begin{aligned} A_{qq,Q}^{\text{NS},(2)} &= \hat{A}_{qq,Q}^{\text{NS},(2)} + (Z_{qq,Q}^{\text{NS}})^{-1,(2)} \\ &= \left\{ -\frac{1}{4} \beta_{0,Q} P_{qq}^{(0)} \right\} \ln^2 \frac{m^2}{\mu^2} + \left\{ -\frac{1}{2} P_{qq,Q}^{\text{NS},(1)} \right\} \ln \frac{m^2}{\mu^2} \\ &\quad + a_{qq,Q}^{\text{NS},(2)} + \frac{1}{4} \beta_{0,Q} \zeta(2) P_{qq}^{(0)}, \end{aligned} \quad (3.35)$$

with

$$\begin{aligned} \left(Z_{qq,Q}^{\text{NS}}\right)^{-1,(2)} &= S_\epsilon^2 \left[ -\frac{1}{\epsilon_{\text{UV}}^2} \beta_{0,Q} P_{qq}^{(0)} + \frac{2}{\epsilon_{\text{UV}}^2} \beta_{0,Q} \left(\frac{m^2}{\mu^2}\right)^{\epsilon/2} \left(1 + \frac{1}{8} \zeta(2) \epsilon_{\text{UV}}^2\right) P_{qq}^{(0)} \right. \\ &\quad \left. + \frac{1}{2\epsilon_{\text{UV}}} P_{qq,Q}^{\text{NS},(1)} \right]. \end{aligned} \quad (3.36)$$

Notice that expressions (3.33) and (3.35) also contribute via (3.28) to the singlet part of the OME.

Since we can infer the coefficients of the double and single pole terms of the unrenormalized OME  $\hat{A}_{ij}$  from the two-loop corrected AP-splitting functions and the beta-function, the above expressions serve as a check on our calculations. The non-pole terms defined by  $a_{ij}^{(2)}$ , which cannot be predicted, have to be calculated in this paper. They are needed to compute the heavy quark coefficient functions (2.18) up to the non-logarithmic term, which will be done in the next section.

Before finishing this section we will give an outline of our calculation of the OME's depicted in figs.1-4. We have computed the OME using the standard QCD Feynman rules and the operator vertices corresponding to (2.24), (2.25) which can be found in the literature (see [17]). Since in our case the latter are S-matrix elements we have to consider the connected Green's functions where the external quark and gluon propagators are amputated. Notice that one has to include the external self energies. The connected Green's function needed for  $A_{qq}$  (figs.1,2) is given by

$$\langle 0 | T(A_\mu^a(x) O_q^{\mu_1 \dots \mu_m}(0) A_\nu^b(y)) | 0 \rangle_c, \quad (3.37)$$

and for  $A_{qq}^{\text{PS}}$  (fig.3) and  $A_{qq}^{\text{NS}}$  (fig.4) we have

$$\langle 0 | T(\bar{\psi}_i(x) O_q^{r,\mu_1 \dots \mu_m}(0) \psi_j(y)) | 0 \rangle_c, \quad (3.38)$$

with  $r = \text{PS}$  and  $r = \text{NS}$  respectively. Further  $a, b$  and  $i, j$  are the colour indices of the gluon field  $A_\mu$  and the quark field  $\psi$  respectively. Since the above operators  $O^{\mu_1 \dots \mu_m}(0)$  are traceless symmetric tensors under the Lorentz group the computation of the connected Green's functions reveals the presence of many trace terms which are not essential for the determination of the anomalous dimensions or splitting functions. Therefore we will project them out by multiplying the operators by an external source  $J_{\mu_1 \dots \mu_m} = \Delta_{\mu_1} \dots \Delta_{\mu_m}$  with



$\Delta^2 = 0$ . Performing the Fourier transform into momentum space and sandwiching the connected Green's functions by the external gluon polarizations and quark spinors one obtains

$$\epsilon^\mu(p) G_{q,\mu\nu}^{ab} \epsilon^\nu(p), \quad (3.39)$$

and

$$\bar{u}(p, s) G_q^{ij} \lambda_r u(p, s), \quad (3.40)$$

where  $\lambda_r$  denote the generators of the flavour group  $SU(n_f)$ . The tensors  $G_{q,\mu\nu}^{ab}$  and  $G_q^{ij}$  have the form

$$G_{q,\mu\nu}^{ab} = \hat{A}_{qq}^{(m)}\left(\epsilon, \frac{m^2}{\mu^2}, \alpha_s\right) \delta^{ab} (\Delta \cdot p)^m \left(-g_{\mu\nu} + \frac{\Delta_\mu p_\nu + \Delta_\nu p_\mu}{\Delta \cdot p}\right), \quad (3.41)$$

and

$$G_q^{ij} = \hat{A}_{qq} \left(\epsilon, \frac{m^2}{\mu^2}, \alpha_s\right) \delta^{ij} (\Delta \cdot p)^{m-1} \not{\Delta}. \quad (3.42)$$

By projecting these tensors out one obtains finally the OME's

$$\hat{A}_{qq}^{(m)}\left(\epsilon, \frac{m^2}{\mu^2}, \alpha_s\right) = \frac{1}{N^2 - 1} \frac{1}{n - 2} (-g_{\mu\nu}) \delta^{ab} (\Delta \cdot p)^{-m} G_{q,\mu\nu}^{ab}, \quad (3.43)$$

$$\hat{A}_{qq}^{(m)}\left(\epsilon, \frac{m^2}{\mu^2}, \alpha_s\right) = \frac{1}{N} \delta^{ij} \frac{1}{4} (\Delta \cdot p)^{-m} \text{Tr}(\not{p} G_q^{ij}). \quad (3.44)$$

Notice that in (3.43) the summation over the dummy indices  $\mu$  and  $\nu$  includes unphysical (non-transverse) gluon polarizations which have to be compensated by adding graphs containing the external ghost lines represented in fig.2s and fig.2t. Instead of  $-g^{\mu\nu}/(n-2)$  one can also use the physical polarization sum  $[-g_{\mu\nu} + (\Delta_\mu p_\nu + \Delta_\nu p_\mu)/\Delta \cdot p]/(n-2)$  and omit the graphs with the external ghost lines. However in this case the individual Feynman graphs lead to integrals with higher powers of the momenta in the numerator so that they become more difficult to compute. Moreover the number of independent integrals is artificially increased. The advantage of constructing the Green's function in the way shown in (3.43), (3.44) is that one does not

have to resort to complicated tensorial reduction programs as had to be used for example in [15]. Therefore one has only Lorentz scalars in the numerators of the Feynman integrals which can be partially cancelled by terms in the denominators. The traces of the fermion loops in figs.1,2 and the contraction with the metric tensor in (3.43) have been performed by using the algebraic manipulation program FORM [22]. We did the same for the graphs in figs.3,4 where we had to compute the trace in (3.44). The computation of the scalar integrals is straightforward as long as the number of propagators does not exceed four. In the case of five different propagators the calculation becomes more cumbersome but here one can use the trick of integration by parts [23]. Examples are given in Appendix B. The results for the unrenormalized OME's are too long to put them in this section and we will defer them to Appendix C.

Apart from the check on the pole terms mentioned above we can also check the finite term of the Abelian part of  $\hat{A}_{Qg}$ . Removing the overall constant  $(1 + (-1)^m)/2$  the Mellin transform reads up to order  $\alpha_s^2$  (see Appendix C)

$$\hat{A}_{Qg}^{(m)} = S_\epsilon \left( \frac{\alpha_s}{4\pi} \right) T_f \left[ \hat{A}_{Qg}^{(1),(m)} \right] + S_\epsilon^2 \left( \frac{\alpha_s}{4\pi} \right)^2 T_f \left[ C_F \hat{A}_{Qg,F}^{(2),(m)} + C_A \hat{A}_{Qg,A}^{(2),(m)} \right]. \quad (3.45)$$

Notice that coupling constant renormalization has already been carried out in the above equation so that we get rid of the term proportional to  $T_f^2$  in (C.1). If we now take the first moment  $m = 1$ ,  $\hat{A}_{Qg,A}^{(2),(m)} \approx (m - 1)^{-1}$  but  $\hat{A}_{Qg}^{(1),(1)}$  and  $\hat{A}_{Qg,F}^{(2),(1)}$  are finite. One can now easily show that there exists a relation between the Abelian terms and the heavy fermion loop contribution to the gluon self energy which we will denote by

$$\hat{\Pi}_V(p^2, m^2) = S_\epsilon \left( \frac{\alpha_s}{4\pi} \right) T_f \hat{\Pi}_V^{(1)}(p^2, m^2) + S_\epsilon^2 \left( \frac{\alpha_s}{4\pi} \right)^2 C_F T_f \hat{\Pi}_V^{(2)}(p^2, m^2). \quad (3.46)$$

The relation is given by

$$\hat{\Pi}_V^{(1)}(0, m^2) = \frac{1}{2} \hat{A}_{Qg}^{(1),(1)}, \quad (3.47)$$

$$\hat{\Pi}_V^{(2)}(0, m^2) = \frac{1}{2} \hat{A}_{Qg,F}^{(2),(1)}. \quad (3.48)$$

$\hat{\Pi}_V^{(1)}(0, m^2)$  and  $\hat{\Pi}_V^{(2)}(0, m^2)$  can be inferred from eqs. (2.11) and (5.1) in [24]. In the latter reference the heavy fermion loop contribution to the self energy of the  $Z$ -boson and the photon were calculated. The self-energy contribution to the gluon and the photon are related as follows

$$\hat{\Pi}_V^{(1)}(p^2, m^2) = 4 \frac{1}{p^2} \Pi_T^V(p^2), \quad (3.49)$$

$$\hat{\Pi}_V^{(2)}(p^2, m^2) = 4^2 \frac{3}{4} \frac{1}{3 p^2} \Pi_T^V(p^2), \quad (3.50)$$

where  $\Pi_T^V(p^2)$  in eqs.(3.49), (3.50) are equal to the expressions quoted in (2.11) and (5.1) of [24] respectively. The factors of 4 originate from the convention that in [24] one expands the quantities in  $\alpha_s/\pi$  instead of  $\alpha_s/(4\pi)$  as is done in this paper. The factors of  $4/3$  and  $3$  refer to the colour factors  $C_F$  and  $C_A$  in  $SU(3)$ . From [24] we infer that

$$\hat{\Pi}_V^{(1)}(0, m^2) = \left(\frac{m^2}{\mu^2}\right)^{\epsilon/2} \left[-\frac{8}{3\epsilon}\right], \quad (3.51)$$

$$\hat{\Pi}_V^{(2)}(0, m^2) = \left(\frac{m^2}{\mu^2}\right)^{\epsilon/2} \left[-\frac{4}{\epsilon} + 15\right], \quad (3.52)$$

where  $n = 4 + \epsilon$ . (Notice that in [24]  $n = 4 - 2\epsilon$ ). Calculation of the first moment of (3.45) (see also (C.1),(C.2)) reveals that the relations in (3.47), (3.48) are satisfied.

## 4 Heavy quark coefficient functions

In this section we will compute the heavy quark coefficient functions  $H_{i,l}$  and  $L_{i,l}$  defined above (2.14) up to order  $\alpha_s^2$  in the asymptotic limit  $Q^2 \gg m^2$ . For this computation we will use the mass factorization theorems as represented by eqs. (2.19) and (2.20) where the transition functions  $\Gamma_{kl}(\mu^2/m^2)$  stand for the finite OME's  $A_{kl}(\mu^2/m^2)$  computed in section 3.

Let us start with the heavy quark coefficient functions which originate from the subprocesses where the virtual photon couples to the heavy quark. Here the mass factorization theorem implies

$$H_{i,l}\left(\frac{Q^2}{m^2}, \frac{\mu^2}{m^2}\right) = A_{kl}\left(\frac{\mu^2}{m^2}\right) \otimes C_{i,k}\left(\frac{Q^2}{\mu^2}\right), \quad (4.1)$$

where  $H_{i,l}$  ( $i = 2, L; l = q, g$ ) denote the heavy quark coefficient functions in the limit  $Q^2 \gg m^2$  and  $A_{kl}$  ( $k, l = q, g$ ) are the finite OME's computed in the last section. The coefficient functions  $C_{i,l}(Q^2/\mu^2)$  have been calculated in [11]. They are obtained from the massless parton structure functions as defined in eqs. (2.27), (2.28), after having performed mass factorization in the  $\overline{\text{MS}}$ -scheme. In the last section also the OME's  $A_{kl}$  have been calculated in the  $\overline{\text{MS}}$ -scheme. In the product on the right-hand-side of (4.1) the scheme dependence is only partially cancelled which is revealed by the fact that  $H_{i,l}$  is still scheme dependent. This dependence, which is indicated by  $\mu^2/m^2$  in  $H_{i,l}$ , originates from the coupling of a light parton (gluon or quark) to an internal light parton characteristic of the production mechanisms of the processes in (2.12) and (2.13).

In the case of the lowest order photon-gluon fusion process we have (see (2.11) and (2.14))

$$H_{L,g}^{(1)}\left(\frac{Q^2}{m^2}, \frac{\mu^2}{m^2}\right) = C_{L,g}^{(1)}\left(\frac{Q^2}{\mu^2}\right), \quad (4.2)$$

$$H_{2,g}^{(1)}\left(\frac{Q^2}{m^2}, \frac{\mu^2}{m^2}\right) = A_{Qg}^{(1)}\left(\frac{\mu^2}{m^2}\right) + C_{2,g}^{(1)}\left(\frac{Q^2}{\mu^2}\right), \quad (4.3)$$

where  $C_{L,g}^{(1)}$ ,  $C_{2,g}^{(1)}$  are the order  $\alpha_s$  gluonic coefficient functions which e.g. can be found in [11]. Like the OME's they can be expressed in the renormalization

group coefficients as

$$C_{L,g}^{(1)}\left(\frac{Q^2}{\mu^2}\right) = c_{L,g}^{(1)}, \quad (4.4)$$

$$C_{2,g}^{(1)}\left(\frac{Q^2}{\mu^2}\right) = \frac{1}{2}P_{qg}^{(0)} \ln \frac{Q^2}{\mu^2} + c_{2,g}^{(1)}. \quad (4.5)$$

From (3.24) and (4.2)-(4.5) one obtains the asymptotic forms for the order  $\alpha_s$  heavy quark coefficient functions

$$H_{L,g}^{(1)}\left(\frac{Q^2}{m^2}, \frac{\mu^2}{m^2}\right) = c_{L,g}^{(1)}, \quad (4.6)$$

$$H_{2,g}^{(1)}\left(\frac{Q^2}{m^2}, \frac{\mu^2}{m^2}\right) = \frac{1}{2}P_{qg}^{(0)} \ln \frac{Q^2}{m^2} + a_{Qg}^{(1)} + c_{2,g}^{(1)}. \quad (4.7)$$

In order  $\alpha_s^2$  the coefficients of the photon-gluon fusion process (2.12) become

$$H_{L,g}^{(2)}\left(\frac{Q^2}{m^2}, \frac{\mu^2}{m^2}\right) = A_{Qg}^{(1)}\left(\frac{\mu^2}{m^2}\right) \otimes C_{L,q}^{(1)}\left(\frac{Q^2}{\mu^2}\right) + C_{L,g}^{(2)}\left(\frac{Q^2}{\mu^2}\right), \quad (4.8)$$

$$H_{2,g}^{(2)}\left(\frac{Q^2}{m^2}, \frac{\mu^2}{m^2}\right) = A_{Qg}^{(2)}\left(\frac{\mu^2}{m^2}\right) + A_{Qg}^{(1)}\left(\frac{\mu^2}{m^2}\right) \otimes C_{2,q}^{(1)}\left(\frac{Q^2}{\mu^2}\right) + C_{2,g}^{(2)}\left(\frac{Q^2}{\mu^2}\right), \quad (4.9)$$

where  $C_{i,q}^{(1)}$ ,  $C_{i,g}^{(2)}$ , ( $i = 2, L$ ) become (see [11])

$$C_{L,q}^{(1)}\left(\frac{Q^2}{\mu^2}\right) = c_{L,q}^{(1)}, \quad (4.10)$$

$$C_{2,q}^{(1)}\left(\frac{Q^2}{\mu^2}\right) = \frac{1}{2}P_{qq}^{(0)} \ln \frac{Q^2}{\mu^2} + c_{2,q}^{(1)}, \quad (4.11)$$

$$C_{L,g}^{(2)}\left(\frac{Q^2}{\mu^2}\right) = \left\{ -\beta_0 c_{L,g}^{(1)} + \frac{1}{2}P_{gg}^{(0)} \otimes c_{L,g}^{(1)} + \frac{1}{2}P_{qg}^{(0)} \otimes c_{L,q}^{(1)} \right\} \ln \frac{Q^2}{\mu^2} + c_{L,g}^{(2)}, \quad (4.12)$$

$$\begin{aligned}
C_{2,g}^{(2)}\left(\frac{Q^2}{\mu^2}\right) &= \left\{ \frac{1}{8}P_{qg}^{(0)} \otimes (P_{gg}^{(0)} + P_{qq}^{(0)}) - \frac{1}{4}\beta_0 P_{qg}^{(0)} \right\} \ln^2 \frac{Q^2}{\mu^2} \\
&+ \left\{ \frac{1}{2}P_{qg}^{(1)} - \beta_0 c_{2,g}^{(1)} + \frac{1}{2}P_{gg}^{(0)} \otimes c_{2,g}^{(1)} + \frac{1}{2}P_{qg}^{(0)} \otimes c_{2,q}^{(1)} \right\} \ln \frac{Q^2}{\mu^2} \\
&+ c_{2,g}^{(2)}. \tag{4.13}
\end{aligned}$$

From (3.24), (3.25) and (4.10)-(4.13) one infers the asymptotic form

$$\begin{aligned}
H_{L,g}^{(2)}\left(\frac{Q^2}{m^2}, \frac{\mu^2}{m^2}\right) &= \left\{ -\beta_0 c_{L,g}^{(1)} + \frac{1}{2}P_{qg}^{(0)} \otimes c_{L,g}^{(1)} + \frac{1}{2}P_{qg}^{(0)} \otimes c_{L,q}^{(1)} \right\} \ln \frac{Q^2}{m^2} \\
&+ \left\{ -\beta_0 c_{L,g}^{(1)} + \frac{1}{2}P_{qg}^{(0)} \otimes c_{L,g}^{(1)} \right\} \ln \frac{m^2}{\mu^2} + c_{L,g}^{(2)} + a_{Qg}^{(1)} \otimes c_{L,q}^{(1)}, \tag{4.14}
\end{aligned}$$

$$\begin{aligned}
H_{2,g}^{(2)}\left(\frac{Q^2}{m^2}, \frac{\mu^2}{m^2}\right) &= \left\{ \frac{1}{8}P_{qg}^{(0)} \otimes (P_{gg}^{(0)} + P_{qq}^{(0)}) - \frac{1}{4}\beta_0 P_{qg}^{(0)} \right\} \ln^2 \frac{Q^2}{m^2} \\
&+ \left\{ \frac{1}{2}P_{qg}^{(1)} - \beta_0 c_{2,g}^{(1)} + \frac{1}{2}P_{qg}^{(0)} \otimes a_{Qg}^{(1)} + \frac{1}{2}P_{gg}^{(0)} \otimes c_{2,g}^{(1)} + \frac{1}{2}P_{qg}^{(0)} \otimes c_{2,q}^{(1)} \right\} \\
&\times \ln \frac{Q^2}{m^2} + \left\{ \frac{1}{4}P_{qg}^{(0)} \otimes P_{gg}^{(0)} - \frac{1}{2}\beta_0 P_{qg}^{(0)} \right\} \ln \frac{Q^2}{m^2} \ln \frac{m^2}{\mu^2} \\
&+ \left\{ -\beta_0 (c_{2,g}^{(1)} + a_{Qg}^{(1)}) + \frac{1}{2}P_{qg}^{(0)} \otimes (c_{2,g}^{(1)} + a_{Qg}^{(1)}) \right\} \ln \frac{m^2}{\mu^2} \\
&+ c_{2,g}^{(2)} + a_{Qg}^{(2)} + 2\beta_0 \bar{a}_{Qg}^{(1)} + c_{2,q}^{(1)} \otimes a_{Qg}^{(1)} + P_{qg}^{(0)} \otimes \bar{a}_{Qg}^{(1)} - P_{gg}^{(0)} \otimes \bar{a}_{Qg}^{(1)}. \tag{4.15}
\end{aligned}$$

Notice that the above formulae are still dependent on the mass factorization and renormalization scale  $\mu^2$ . The same scale dependence was also found for the exact expressions for the heavy quark coefficient functions where  $Q^2$  and  $m^2$  can be arbitrarily chosen. The  $\mu^2$  dependence can be attributed to coupling constant renormalization represented by the lowest order coefficient  $\beta_0$  in the beta-function and the lowest order splitting function  $P_{qg}^{(0)}$  standing for the transition  $g \rightarrow g + g$ .

The computation of the asymptotic expression of the heavy quark coefficient function corresponding to the Bethe-Heitler process (2.13) proceeds in the same way. From (4.1) we derive

$$H_{L,q}^{(2)}\left(\frac{Q^2}{m^2}, \frac{\mu^2}{m^2}\right) = C_{L,q}^{\text{PS},(2)}\left(\frac{Q^2}{\mu^2}\right), \tag{4.16}$$

$$H_{2,q}^{(2)}\left(\frac{Q^2}{m^2}, \frac{\mu^2}{m^2}\right) = A_{Qq}^{\text{PS},(2)}\left(\frac{\mu^2}{m^2}\right) + C_{2,q}^{\text{PS},(2)}\left(\frac{Q^2}{\mu^2}\right). \quad (4.17)$$

The coefficient functions  $C_{i,q}^{\text{PS},(2)}$  ( $i = 2, L$ ) are computed in [11] and they read

$$C_{L,q}^{\text{PS},(2)}\left(\frac{Q^2}{\mu^2}\right) = \left\{\frac{1}{2}P_{gq}^{(0)} \otimes c_{L,g}^{(1)}\right\} \ln \frac{Q^2}{\mu^2} + c_{L,q}^{\text{PS},(2)}, \quad (4.18)$$

$$\begin{aligned} C_{2,q}^{\text{PS},(2)}\left(\frac{Q^2}{\mu^2}\right) &= \left\{\frac{1}{8}P_{gq}^{(0)} \otimes P_{gq}^{(0)}\right\} \ln^2 \frac{Q^2}{\mu^2} + \left\{\frac{1}{2}P_{qq}^{\text{PS},(1)} + \frac{1}{2}P_{gq}^{(0)} \otimes c_{2,g}^{(1)}\right\} \ln \frac{Q^2}{\mu^2} \\ &\quad + c_{2,q}^{\text{PS},(2)}. \end{aligned} \quad (4.19)$$

Using (3.31) and (4.18), (4.19) the heavy quark coefficient functions become

$$\begin{aligned} H_{L,q}^{(2)}\left(\frac{Q^2}{m^2}, \frac{\mu^2}{m^2}\right) &= \left\{\frac{1}{2}P_{gq}^{(0)} \otimes c_{L,g}^{(1)}\right\} \ln \frac{Q^2}{m^2} + \left\{\frac{1}{2}P_{gq}^{(0)} \otimes c_{L,g}^{(1)}\right\} \ln \frac{m^2}{\mu^2} \\ &\quad + c_{L,q}^{\text{PS},(2)}, \end{aligned} \quad (4.20)$$

$$\begin{aligned} H_{2,q}^{(2)}\left(\frac{Q^2}{m^2}, \frac{\mu^2}{m^2}\right) &= \left\{\frac{1}{8}P_{gq}^{(0)} \otimes P_{gq}^{(0)}\right\} \ln^2 \frac{Q^2}{m^2} + \left\{\frac{1}{2}P_{qq}^{\text{PS},(1)} + \frac{1}{2}P_{gq}^{(0)} \otimes c_{2,g}^{(1)}\right\} \\ &\quad \times \ln \frac{Q^2}{m^2} + \left\{\frac{1}{4}P_{gq}^{(0)} \otimes P_{gq}^{(0)}\right\} \ln \frac{Q^2}{m^2} \ln \frac{m^2}{\mu^2} \\ &\quad + \left\{\frac{1}{2}P_{gq}^{(0)} \otimes (c_{2,g}^{(1)} + a_{Qg}^{(1)})\right\} \ln \frac{m^2}{\mu^2} \\ &\quad + c_{2,q}^{\text{PS},(2)} + a_{Qq}^{\text{PS},(2)} - P_{gq}^{(0)} \otimes \bar{a}_{Qg}^{(1)}. \end{aligned} \quad (4.21)$$

Notice that the above  $\mu^2$ -dependence can be only attributed to the mass factorization scheme which enters via the transition  $q \rightarrow g + q$  represented by the splitting function  $P_{gq}^{(0)}$ . The mass factorization for the heavy quark coefficient functions where the photon couples to the light quark proceeds in a similar way as given in eq.(4.1) i.e.,

$$L_{i,l}\left(\frac{Q^2}{m^2}, \frac{\mu^2}{m^2}\right) = A_{kl}\left(\frac{\mu^2}{m^2}\right) \otimes C_{i,k}\left(\frac{Q^2}{\mu^2}\right). \quad (4.22)$$

In the case of the Compton process (2.13) where  $L_{i,q}$  is of order  $\alpha_s^2$  one can derive

$$L_{L,q}^{\text{NS,(2)}}\left(\frac{Q^2}{m^2}, \frac{\mu^2}{m^2}\right) = C_{L,q,f}^{\text{NS,(2)}}\left(\frac{Q^2}{\mu^2}\right), \quad (4.23)$$

$$L_{2,q}^{\text{NS,(2)}}\left(\frac{Q^2}{m^2}, \frac{\mu^2}{m^2}\right) = A_{qq,f}^{\text{NS,(2)}}\left(\frac{\mu^2}{m^2}\right) + C_{2,q,f}^{\text{NS,(2)}}\left(\frac{Q^2}{\mu^2}\right), \quad (4.24)$$

where  $C_{i,q,f}^{\text{NS,(2)}}$  ( $i = 2, L$ ) denotes the quark loop contribution to the non-singlet coefficient function for one specific massless flavour  $f$  which is given by (see [11])

$$C_{L,q,f}^{\text{NS,(2)}}\left(\frac{Q^2}{\mu^2}\right) = \left\{ -\beta_{0,f} c_{L,q}^{(1)} \right\} \ln \frac{Q^2}{\mu^2} + c_{L,q,f}^{\text{NS,(2)}}, \quad (4.25)$$

$$\begin{aligned} C_{2,q,f}^{\text{NS,(2)}}\left(\frac{Q^2}{\mu^2}\right) &= \left\{ -\frac{1}{4}\beta_{0,f} P_{qq}^{(0)} \right\} \ln^2 \frac{Q^2}{\mu^2} + \left\{ \frac{1}{2}P_{qq,f}^{\text{NS,(1)}} - \beta_{0,f} c_{2,q}^{(1)} \right\} \ln \frac{Q^2}{\mu^2} \\ &\quad + c_{2,q,f}^{\text{NS,(2)}}. \end{aligned} \quad (4.26)$$

Notice that the above coefficient functions are represented in the  $\overline{\text{MS}}$ -scheme for the coupling constant renormalization (see (3.6)). However  $A_{qq}^{\text{NS,(2)}}$  in (3.35) has been determined in another scheme where the heavy flavour  $Q$  decouples in the strong coupling constant (see (3.7)). Choosing the latter scheme and putting  $f = Q$  we obtain instead of (4.25), (4.26) the expressions

$$C_{i,q,f}^{\text{NS,(2)}}\left(\frac{Q^2}{\mu^2}, \frac{\mu^2}{m^2}\right) = C_{i,q,f}^{\text{NS,(2)}}\left(\frac{Q^2}{\mu^2}\right) + \left\{ \beta_{0,Q} c_{i,q}^{(1)} \right\} \ln \frac{m^2}{\mu^2}, \quad (4.27)$$

with  $C_{i,q}^{(1)}$  defined in (4.10), (4.11). Substitution of (4.27) and (3.35) in equations (4.23), (4.24) yields the following heavy flavour coefficient functions

$$L_{L,q}^{\text{NS,(2)}}\left(\frac{Q^2}{m^2}, \frac{\mu^2}{m^2}\right) = \left\{ -\beta_{0,Q} c_{L,q}^{(1)} \right\} \ln \frac{Q^2}{m^2} + c_{L,q,Q}^{\text{NS,(2)}}, \quad (4.28)$$

$$\begin{aligned} L_{2,q}^{\text{NS,(2)}}\left(\frac{Q^2}{m^2}, \frac{\mu^2}{m^2}\right) &= \left\{ -\frac{1}{4}\beta_{0,Q} P_{qq}^{(0)} \right\} \ln^2 \frac{Q^2}{m^2} + \left\{ \frac{1}{2}P_{qq,Q}^{\text{NS,(1)}} - \beta_{0,Q} c_{2,q}^{(1)} \right\} \ln \frac{Q^2}{m^2} \\ &\quad + c_{2,q,Q}^{\text{NS,(2)}} + a_{qq,Q}^{\text{NS,(2)}} + \frac{1}{4}\beta_{0,Q} \zeta(2) P_{qq}^{(0)}. \end{aligned} \quad (4.29)$$



Notice that in the above expressions the  $\mu^2$ -dependence has completely disappeared due to the special choice of the coupling constant renormalization scheme.

Since we have now all renormalization group coefficients at hand we can calculate the heavy quark coefficient functions  $H_{k,i}$  and  $L_{k,i}$  in the asymptotic limit  $Q^2 \gg m^2$  for arbitrary  $z$ . The splitting functions  $P_{ij}^{(0)}$ ,  $P_{ij}^{(1)}$  and the nonpole terms in the OME's  $a_{ij}^{(1)}$ ,  $a_{ij}^{(2)}$  ( $i, j = q, g$ ) were presented in section 3. The coefficients  $c_{L,i}^{(k)}$ ,  $c_{2,i}^{(k)}$  ( $k = 1, 2$ ;  $i = q, g$ ) appearing in the light quark and gluon deep inelastic coefficient functions can be found in Appendix B of [11] (see also Appendix B in [25]). The analytic expressions for eqs. (4.14), (4.15), (4.20), (4.21), (4.28), (4.29) are too long to be presented here and one can find them in Appendix D.

Before finishing this section we want to study the behaviour of the coefficient functions  $H_{k,i}(z, Q^2/m^2, \mu^2/m^2)$  ( $k = 2, L$ ;  $i = q, g$ ) in the limit  $z \rightarrow 0$ , or  $\eta \rightarrow \infty$ . The behaviour of these functions for  $z = 0$  at arbitrary  $Q^2$  has been predicted in [26] based on the method of  $k_t$ -factorization. Using the notations in [12] we have the following predictions from [26]

$$\lim_{z \rightarrow 0} H_{L,i}^{(2)}\left(z, \xi, \frac{\mu^2}{m^2}\right) = \frac{1}{z} 16\pi C_i T_f \xi \left[ G_L(\eta, \xi) + \bar{G}_L(\eta, \xi) \ln \frac{\mu^2}{m^2} \right], \quad (4.30)$$

$$\begin{aligned} \lim_{z \rightarrow 0} H_{2,i}^{(2)}\left(z, \xi, \frac{\mu^2}{m^2}\right) &= \frac{1}{z} 16\pi C_i T_f \xi \left[ G_T(\eta, \xi) + \bar{G}_L(\eta, \xi) \right. \\ &\quad \left. + \{ \bar{G}_T(\eta, \xi) + \bar{G}_L(\eta, \xi) \} \ln \frac{\mu^2}{m^2} \right], \end{aligned} \quad (4.31)$$

with  $i = q, g$  and  $C_q = C_F$ ,  $C_g = C_A$  and  $\eta, \xi$  are defined in (2.17). The functions  $G_k(\eta, \xi)$ ,  $\bar{G}_k(\eta, \xi)$  ( $k = L, T$ ) are given by eqs.(19)-(24) in [12] for arbitrary  $\xi$ . In the limit  $\xi \rightarrow \infty$  they behave like

$$\lim_{\xi \rightarrow \infty} G_L(\eta, \xi) = \frac{1}{6\pi} \frac{1}{\xi} \left[ 4 \ln \xi - \frac{4}{3} \right], \quad (4.32)$$

$$\lim_{\xi \rightarrow \infty} G_T(\eta, \xi) = \frac{1}{6\pi} \frac{1}{\xi} \left[ 2 \ln^2 \xi + \frac{14}{3} \ln \xi - 4\zeta(2) + \frac{14}{3} \right], \quad (4.33)$$

$$\lim_{\xi \rightarrow \infty} \bar{G}_L(\eta, \xi) = \frac{1}{6\pi} \frac{1}{\xi} [-4], \quad (4.34)$$

$$\lim_{\xi \rightarrow \infty} \bar{G}_T(\eta, \xi) = \frac{1}{6\pi} \frac{1}{\xi} [-4 \ln \xi + 2]. \quad (4.35)$$

Substitution of the above equations into (4.30) and (4.31) yields the asymptotic behaviour

$$\lim_{z \rightarrow 0} H_{L,i}^{(2)}(z, \xi, \frac{\mu^2}{m^2}) = \frac{1}{z} C_i T_f \left[ \frac{32}{3} \ln \xi + \frac{32}{3} \ln \frac{m^2}{\mu^2} - \frac{32}{9} \right], \quad (4.36)$$

$$\begin{aligned} \lim_{z \rightarrow 0} H_{2,i}^{(2)}(z, \xi, \frac{\mu^2}{m^2}) &= \frac{1}{z} C_i T_f \left[ \frac{16}{3} \ln^2 \xi + \left( \frac{32}{3} \ln \frac{m^2}{\mu^2} + \frac{208}{9} \right) \ln \xi \right. \\ &\quad \left. + \frac{16}{3} \ln \frac{m^2}{\mu^2} - \frac{32}{3} \zeta(2) + \frac{80}{9} \right], \end{aligned} \quad (4.37)$$

which agrees with expressions (D.3)-(D.6) in the limit  $z \rightarrow 0$ .

## 5 Results

In this section we want to make a comparison between the exact heavy quark coefficient functions in [3] and the asymptotic ones derived in this paper. The exact coefficient functions which are either available in computer programs [3] or in tables [12] were defined in the latter references using the notation  $c_{k,i}^{(l)}$ ,  $\bar{c}_{k,i}^{(l)}$  ( $k = 2, L; i = q, \bar{q}, g; l = 0, 1$ ) and  $d_{k,i}^{(1)}$ . These twelve coefficient functions are related to the  $H_{k,i}^{(l)}$  in (2.14), (2.15) and  $L_{k,i}^{(l)}$  (2.16) defined in this paper as follows. For the Born reaction we have the identity

$$H_{k,g}^{(1)}(z, \xi) = \frac{1}{\pi} \frac{\xi}{z} c_{k,g}^{(0)}(\eta, \xi), \quad (5.1)$$

with  $\eta$  and  $\xi$  defined in (2.17). For the gluon-fusion process in (2.12) and the Bethe-Heitler process (2.13) we have

$$H_{k,i}^{(2)}\left(z, \xi, \frac{\mu^2}{m^2}\right) = 16\pi \frac{\xi}{z} [c_{k,i}^{(1)}(\eta, \xi) + \bar{c}_{k,i}^{(1)}(\eta, \xi) \ln \frac{\mu^2}{m^2}], \quad (5.2)$$

and for the Compton process (2.13) one has

$$L_{k,q}^{(2)}\left(z, \xi, \frac{\mu^2}{m^2}\right) = 16\pi \frac{\xi}{z} d_{k,q}^{(1)}(\eta, \xi). \quad (5.3)$$

The exact coefficient functions were plotted in figures 6-11 in [3] as functions of  $\eta$  for various values of  $\xi$ . Here we want to show at which  $\xi$  values the asymptotic forms of the coefficient functions presented in section 4 give a good approximation of the ones derived in [3].

We do not need to discuss the lowest order coefficient functions  $c_{L,g}^{(0)}$  and  $c_{2,g}^{(0)}$  as they have a very simple analytic form. The same is true for the coefficients of the mass factorization logarithms,  $\bar{c}_{L,g}^{(1)}$ ,  $\bar{c}_{2,g}^{(1)}$ ,  $\bar{c}_{L,q}^{(1)}$  and  $\bar{c}_{2,q}^{(1)}$ . Therefore we concentrate on the asymptotic values of the NLO coefficient functions and start by defining the ratios  $R_{k,i}^{(1)}$  and  $T_{k,i}^{(1)}$  which are given by

$$R_{k,i}^{(1)}(z, \xi) = \frac{c_{k,i}^{(1)}(z, \xi)}{c_{k,i}^{(1),\text{asympt}}(z, \xi)}, \quad (5.4)$$

and

$$T_{k,i}^{(1)}(z, \xi) = \frac{d_{k,i}^{(1)}(z, \xi)}{d_{k,i}^{(1),\text{asympt}}(z, \xi)}. \quad (5.5)$$

Here  $c_{k,i}^{(1),\text{asympt}}(z, \xi)$  and  $d_{k,q}^{(1),\text{asympt}}(z, \xi)$  are the asymptotic expressions for the heavy quark coefficient functions derived in section 4 in the limit  $\xi \rightarrow \infty$ . In this paper the above ratios will only be presented for charm production at the HERA collider on account of the small value of the charm mass and the  $Q^2$  values accessible. Choosing the range  $5 < \xi < 10^5$  we will study the above ratios for  $z = 10^{-2}$  and  $10^{-4}$ .

In fig.5 we show  $R_{L,g}^{(1)}$  (5.4) and it is apparent that the asymptotic formula coincides with the exact NLO result when  $\xi \geq 10^3$ . There is essentially no difference between the ratios for  $z = 10^{-2}$  and  $10^{-4}$ . However if  $z = 10^{-4}$  the exact calculation begins to show computer instabilities when  $\xi \geq 10^4$  so we did not run at larger values.

The next figure fig.6 shows  $R_{2,g}^{(1)}$  and we deduce that our approximate formula is good for  $\xi \geq 10$ . This value is much lower than the one observed for  $R_{L,g}^{(1)}$  which shows that the asymptotic limit is reached much faster for  $H_{2,g}^{(2)}$  than for  $H_{L,g}^{(2)}$ . Furthermore the lower bound is independent of our choice of  $z$ . The scatter in fig. 6 at large values of  $\xi$  reflects the numerical errors in the computer program of the exact NLO result in [12]. This numerical uncertainty is therefore one of the reasons why we derived the asymptotic formulae for the heavy quark coefficient functions in this paper.

Continuing with these ratios we plot  $R_{L,q}^{(1)}$  versus  $\xi$  in fig.7. There is not much difference between  $R_{L,q}^{(1)}$  and  $R_{L,g}^{(1)}$  (see fig. 5) . The asymptotic formula for the quark channel is good for  $\xi \geq 10^3$  for both values of  $z$ . A similar observation holds for  $R_{2,q}^{(1)}$  in Fig.8 when compared with  $R_{2,g}^{(1)}$  in fig. 6. Like in the latter case the exact formula approaches the exact one when  $\xi \geq 10$ .

Finally we turn to the ratios  $T_{k,q}^{(1)}$  (5.5) in Fig.9. Here we have used the exact NLO formulae for  $L_{k,q}^{(2)}$  (5.3) presented in Appendix A rather than computing them from the program in [12]. This is the reason we have no numerical troubles at very large  $\xi$ . In fig. 9 and fig. 10 we have plotted  $T_{L,q}^{(1)}$  and  $T_{2,q}^{(1)}$  respectively. From these figures we infer that at small  $z$  ( here  $z = 10^{-4}$  ) the asymptotic formulae coincide with the exact ones over the whole  $\xi$ -range. At larger  $z$ -values (e.g. at  $z = 10^{-2}$ ) the approximation gets worse and it becomes only good when  $\xi \geq 10^2$ .

Before drawing any conclusions about the validity of our asymptotic expressions one has to bear the following in mind. First of all the heavy quark coefficient functions have to be convoluted with the parton densities according to (2.8) in order to obtain the charm contributions to the deep inelastic

structure functions. Therefore there are parts of the integration region over  $z$  which can become more important than some other ones. Second the lower bounds on the  $\xi$ -values given above have to be viewed in the mathematical rather than in the physical sense. Experimentally the structure function  $F_2(x, Q^2, m_c^2)$  will become much better determined than the longitudinal one given by  $F_L(x, Q^2, m_c^2)$ . In the latter case we are already glad that it can be measured up to 20 – 30% accuracy. Furthermore in this paper we are dealing with NLO corrections which have to be less precise than the Born approximation. Also the contribution coming from the Compton subprocess leading to the plots in figs. 9,10 is much smaller than the one originating from the photon-gluon fusion reaction for which the ratios  $R_{k,g}^{(1)}$  are plotted in figs. 5,6. Therefore the physical bounds on  $\xi$  can be put much smaller than the ones given above. In view of the theoretical and experimental uncertainties we can state that the asymptotic formulae for the heavy flavour coefficient functions can be used when  $\xi \geq 4$  in the case of  $F_2$  whereas  $\xi \geq 10$  is good enough for  $F_L$ .

To summarize the calculations presented in this paper we have used the OPE techniques and the renormalization group equations to find analytic formulae for the asymptotic behaviour ( $\xi \gg 1$ ) of the heavy flavour coefficient functions which enter in deep inelastic electroproduction. We have tested these asymptotic formulae against the exact NLO results in our rather complicated computer programs and find good agreement when  $\xi \geq 4$  for  $F_2$  and  $\xi \geq 10$  in the case of  $F_L$ . Below these values our asymptotic formulae fail and one has to use the exact NLO computer programs to compute the heavy quark coefficient functions.

Acknowledgements.

The work of Y. Matiounine and J. Smith was supported in part under the contract NSF 93-09888. R. Migneron would like to thank the Netherlands Organization for Scientific Research (NWO) for financial support.

## Appendix A

In this Appendix we present the exact expressions for the heavy quark coefficient functions  $L_{i,q}^{(2)}$  (2.16) corresponding to the Compton reaction (2.13). The calculation is straightforward because one can first integrate over the heavy quark momenta in the final state without affecting the momentum of the remaining light quark (see figs. 5c,d in [3]). The phase space integrals are then the same as the ones obtained for the process  $\gamma^* + q \rightarrow g^* + q$  ( $g^* \rightarrow Q + \bar{Q}$ ) where the gluon  $g^*$  becomes virtual. After integration over the virtual mass of the gluon one gets the expressions

$$\begin{aligned}
L_{L,q}^{(2)}(z, Q^2, m^2) = & C_F T_f \left[ 96z \left(\frac{z}{\xi}\right)^2 \left\{ \ln\left(\frac{1-z}{z^2}\right) L_1 + L_1 L_2 + 2(-DIL_1 \right. \right. \\
& + DIL_2 + DIL_3 - DIL_4) \left. \left. \right\} + \left(\frac{z}{(1-z)\xi}\right)^2 (64 - 288z + 192z^2) L_1 \right. \\
& + z \left\{ \frac{16}{3} - \frac{416}{3} \left(\frac{z}{\xi}\right) + \frac{1408}{3} \left(\frac{z}{\xi}\right)^2 \right\} \frac{L_3}{sq_2} + \left\{ \frac{16}{3} - \frac{400}{18} z + \left(\frac{z}{(1-z)\xi}\right) \right. \\
& \left. \left. \times \left(-\frac{160}{3} + \frac{3824}{9} z - \frac{992}{3} z^2\right) \right\} sq_1 \right], \tag{1.1}
\end{aligned}$$

$$\begin{aligned}
L_{2,q}^{(2)}(z, Q^2, m^2) = & C_F T_f \left[ \left\{ \frac{4}{3} \frac{1+z^2}{1-z} - \frac{16}{1-z} \left(\frac{z}{\xi}\right)^2 (1 - 9z + 9z^2) \right\} \right. \\
& \times \left\{ \ln\left(\frac{1-z}{z^2}\right) L_1 + L_1 L_2 + 2(-DIL_1 + DIL_2 + DIL_3 - DIL_4) \right\} \\
& + \left\{ -\frac{8}{3} + \frac{4}{1-z} + \left(\frac{z}{(1-z)\xi}\right)^2 (128 - 432z + 288z^2 - \frac{8}{1-z}) \right\} L_1 \\
& + \left\{ \frac{88}{9} + \frac{136}{9} z - \frac{152}{9} \frac{1}{1-z} + \left(\frac{z}{(1-z)\xi}\right) \left(\frac{464}{9} - \frac{512}{3} z + \frac{2048}{9} z^2\right) \right. \\
& + \left. \left(\frac{z}{(1-z)\xi}\right)^2 \left(-\frac{832}{9} + \frac{6208}{9} z - \frac{11392}{9} z^2 + \frac{6016}{9} z^3\right) \right\} \frac{L_3}{sq_2} \\
& + \left\{ -\frac{272}{27} - \frac{1244}{27} z + \frac{718}{27} \frac{1}{1-z} + \left(\frac{z}{(1-z)\xi}\right) \left(-\frac{3424}{27} + \frac{15608}{27} z \right. \right. \\
& \left. \left. - \frac{4304}{9} z^2 + \frac{20}{27} \frac{1}{1-z} \right) \right\} sq_1 \right], \tag{1.2}
\end{aligned}$$

where  $\xi = Q^2/m^2$  (2.17). Further we have defined

$$sq_1 = \sqrt{1 - 4\frac{z}{\xi}} \quad , \quad sq_2 = \sqrt{1 - 4\frac{z}{(1-z)\xi}} \quad , \quad (1.3)$$

$$L_1 = \ln\left(\frac{1 + sq_1}{1 - sq_1}\right) \quad , \quad L_2 = \ln\left(\frac{1 + sq_2}{1 - sq_2}\right) \quad , \quad L_3 = \ln\left(\frac{sq_2 + sq_1}{sq_2 - sq_1}\right) \quad , \quad (1.4)$$

$$DIL_1 = \text{Li}_2\left(\frac{(1-z)(1 + sq_1)}{1 + sq_2}\right) \quad , \quad DIL_2 = \text{Li}_2\left(\frac{1 - sq_2}{1 + sq_1}\right) \quad , \quad (1.5)$$

$$DIL_3 = \text{Li}_2\left(\frac{1 - sq_1}{1 + sq_2}\right) \quad , \quad DIL_4 = \text{Li}_2\left(\frac{1 + sq_1}{1 + sq_2}\right) \quad , \quad (1.6)$$

with  $0 < z < \xi/(\xi + 4)$ .

## Appendix B

Here we apply the method of integration by parts which enables us to reduce scalar two-loop OME integrals with five different propagators to expressions containing only four different propagators. The method is a generalization of the trick invented in [23] where it was used to reduce two-loop self-energy integrals with five different propagators to integrals which only contain four different propagators.

Feynman integrals with five different propagators emerge from the computation of the graphs  $e, f, h, l, m, n, o$  in fig. 2. Let us first start with graphs 2l, 2o which lead to the following expression

$$I^{(m)} = \int \frac{d^n q}{(2\pi)^n} \int \frac{d^n k}{(2\pi)^n} \frac{(\Delta \cdot q)^m}{D_k D_q^a D_{kp} D_{qp} D_{kq}}, \quad (2.1)$$

where  $a$  is 1 or 2. The denominators are defined as

$$D_k = k^2 - m_1^2, \quad (2.2)$$

$$D_q = q^2 - m_2^2, \quad (2.3)$$

$$D_{kp} = (k - p)^2 - m_3^2, \quad (2.4)$$

$$D_{qp} = (q - p)^2 - m_4^2, \quad (2.5)$$

$$D_{kq} = (k - q)^2 - m_5^2. \quad (2.6)$$

In  $n$ -dimensional regularization the following integral is zero

$$0 = \int \frac{d^n q}{(2\pi)^n} \int \frac{d^n k}{(2\pi)^n} \frac{\partial}{\partial k_\mu} \left[ \frac{k_\mu (\Delta \cdot q)^m}{D_k D_q^a D_{kp} D_{qp} D_{kq}} \right]. \quad (2.7)$$

Differentiating the right-hand-side of (B.7) we obtain

$$0 = nI^{(m)} + \int \frac{d^n q}{(2\pi)^n} \int \frac{d^n k}{(2\pi)^n} \frac{(\Delta \cdot q)^m}{D_k D_q^a D_{kp} D_{qp} D_{kq}} \left\{ -\frac{2k^2}{D_k} - \frac{2k \cdot (k - p)}{D_{kp}} - \frac{2k \cdot (k - q)}{D_{kq}} \right\}. \quad (2.8)$$



In the case that the following conditions are satisfied i.e.,  $m_1 = 0$ ,  $p^2 = m_1^2 + m_3^2$ ,  $m_2^2 = m_1^2 + m_5^2$  one can write

$$-2k \cdot (k - p) = -D_k - D_{kp}, \quad (2.9)$$

$$-2k \cdot (k - q) = -D_k - D_{kq} + D_q. \quad (2.10)$$

Substitution of (B.9) and (B.10) into (B.8) yields

$$\begin{aligned} I^{(m)} &= \frac{1}{n-4} \int \frac{d^n q}{(2\pi)^n} \int \frac{d^n k}{(2\pi)^n} (\Delta \cdot q)^m \left\{ \frac{1}{D_q^a D_{kp}^2 D_{qp} D_{kq}} \right. \\ &\quad \left. + \frac{1}{D_q^a D_{kp} D_{qp} D_{kq}^2} - \frac{1}{D_k D_q^{a-1} D_{kp} D_{qp} D_{kq}^2} \right\}. \end{aligned} \quad (2.11)$$

If  $a = 1$  we have already reached our goal. When  $a = 2$  we have to repeat the trick for the last term in (B.11) so that we finally get

$$\begin{aligned} I^{(m)} &= \frac{1}{n-4} \int \frac{d^n q}{(2\pi)^n} \int \frac{d^n k}{(2\pi)^n} (\Delta \cdot q)^m \left[ \frac{1}{D_q^a D_{kp}^2 D_{qp} D_{kq}} \right. \\ &\quad \left. + \frac{1}{D_q^a D_{kp} D_{qp} D_{kq}^2} - \frac{1}{n-5} \left\{ \frac{1}{D_q^{a-1} D_{kp}^2 D_{qp} D_{kq}^2} \right. \right. \\ &\quad \left. \left. + \frac{2}{D_q^{a-1} D_{kp} D_{qp} D_{kq}^3} - \frac{2}{D_k D_q^{a-2} D_{kp} D_{qp} D_{kq}^3} \right\} \right]. \end{aligned} \quad (2.12)$$

For graphs  $2e, 2h$  we have to differentiate as follows

$$\begin{aligned} 0 &= \int \frac{d^n q}{(2\pi)^n} \int \frac{d^n k}{(2\pi)^n} \frac{\partial}{\partial k_\mu} \left[ \frac{(k-q)_\mu (\Delta \cdot q)^m}{D_k D_q^a D_{kp} D_{qp} D_{kq}} \right] \\ &= n I^{(m)} + \int \frac{d^n q}{(2\pi)^n} \frac{d^n k}{(2\pi)^n} \frac{(\Delta \cdot q)^m}{D_k D_q^a D_{kp} D_{qp} D_{kq}} \\ &\quad \times \left\{ -\frac{2k \cdot (k-q)}{D_k} - \frac{2(k-q) \cdot (k-p)}{D_{kp}} - \frac{2(k-q)^2}{D_{kq}} \right\}. \end{aligned} \quad (2.13)$$

Imposing the following conditions  $m_5 = 0$ ,  $m_2^2 = m_1^2 + m_5^2$ ,  $m_4^2 = m_3^2 + m_5^2$  one gets identity (B.10) and

$$-2(k-q) \cdot (k-p) = D_{qp} - D_{kq} - D_{kp} \quad (2.14)$$

so that  $I^{(m)}$  equals

$$I^{(m)} = \frac{1}{n-4} \int \frac{d^n q}{(2\pi)^n} \int \frac{d^n k}{(2\pi)^n} (\Delta \cdot q)^m \left[ \frac{1}{D_k^2 D_q^a D_{kp} D_{qp}} + \frac{1}{D_k D_q^a D_{kp}^2 D_{qp}} - \frac{1}{D_k D_q^a D_{kp}^2 D_{kq}} - \frac{1}{D_k^2 D_q^{a-1} D_{kp} D_{qp} D_{kq}} \right]. \quad (2.15)$$

For  $a = 1$  we have already four different propagators. If  $a = 2$  one has to repeat the trick again analogous to (B.11).

The trick of integration by parts also applies to graph  $2m$ . For this graph we have the integral

$$J^{(m)} = \int \frac{d^n q}{(2\pi)^n} \int \frac{d^n k}{(2\pi)^n} \frac{(\Delta \cdot q)^m}{D_k D_q^a D_{kp} D_{kq} D_{kqp}}, \quad (2.16)$$

with

$$D_{kqp} = (k - q - p)^2 - m_6^2. \quad (2.17)$$

Performing the differentiation with respect to  $k$  in the same way as in (B.7) one obtains

$$J^{(m)} = \frac{1}{n-4} \int \frac{d^n q}{(2\pi)^n} \int \frac{d^n k}{(2\pi)^n} (\Delta \cdot q)^m \left[ \frac{1}{D_q^a D_{kp}^2 D_{kq} D_{kqp}} + \frac{1}{D_q^a D_{kp} D_{kq}^2 D_{kqp}} + \frac{1}{D_k D_q^a D_{kp} D_{kqp}^2} + \frac{1}{D_k D_q^a D_{kq} D_{kqp}^2} - \frac{1}{D_k D_q^{a-1} D_{kp} D_{kq}^2 D_{kqp}} - \frac{1}{D_k D_q^{a-1} D_{kq} D_{kp} D_{kqp}^2} \right]. \quad (2.18)$$

In the above expression we have used the relations in (B.9), (B.10) and

$$-2k \cdot (k - q - p) = D_q - D_{kq} - D_{kp}, \quad (2.19)$$

which only holds under the conditions  $p^2 = m_3^2$ ,  $m_1^2 = 0$ ,  $m_2^2 = m_5^2$ .

The integrals corresponding to graphs  $2f$  and  $2n$  need some special treatment because of the sum  $\sum_{i=0}^m (\Delta \cdot k)^i (\Delta \cdot q)^{m-i}$  which appears in the operator vertex. Notice that this sum also appears in graphs  $2h$ ,  $2o$  but after some

rearrangement of terms it drops out of the integrals. For graph  $2n$  we have the expression

$$K^{(m)} = \int \frac{d^n q}{(2\pi)^n} \int \frac{d^n k}{(2\pi)^n} \frac{(\Delta \cdot k)^m - (\Delta \cdot q)^m}{(\Delta \cdot k - \Delta \cdot q)} \frac{1}{D_q D_k D_{kp} D_{kq} D_{kqp}}, \quad (2.20)$$

with  $m_1^2 = m_2^2 = m_3^2 = m^2$  and  $m_5^2 = m_6^2 = 0$ . The integral  $K^{(m)}$  can be split into  $K^{(m)} = K_1^{(m)} - K_2^{(m)}$  with

$$K_1^{(m)} = \int \frac{d^n q}{(2\pi)^n} \int \frac{d^n k}{(2\pi)^n} \frac{(\Delta \cdot k)^m}{(\Delta \cdot k - \Delta \cdot q)} \frac{1}{D_q D_k D_{kp} D_{kq} D_{kqp}}, \quad (2.21)$$

$$K_2^{(m)} = \int \frac{d^n q}{(2\pi)^n} \int \frac{d^n k}{(2\pi)^n} \frac{(\Delta \cdot q)^m}{(\Delta \cdot k - \Delta \cdot q)} \frac{1}{D_q D_k D_{kp} D_{kq} D_{kqp}}. \quad (2.22)$$

Differentiating the integrand in (B.21) with respect to  $q$  and (B.22) with respect to  $k$  analogous to (B.13) we obtain

$$\begin{aligned} K_1^{(m)} &= \frac{1}{n-5} \int \frac{d^n q}{(2\pi)^n} \int \frac{d^n k}{(2\pi)^n} \frac{(\Delta \cdot k)^m}{(\Delta \cdot k - \Delta \cdot q)} \left[ \frac{1}{D_k D_q^2 D_{kp} D_{kqp}} \right. \\ &\quad \left. + \frac{1}{D_k D_q D_{kp} D_{kqp}^2} - \frac{1}{D_q^2 D_{kp} D_{kq} D_{kpq}} \right], \end{aligned} \quad (2.23)$$

$$\begin{aligned} K_2^{(m)} &= \frac{1}{n-5} \int \frac{d^n q}{(2\pi)^n} \int \frac{d^n k}{(2\pi)^n} \frac{(\Delta \cdot q)^m}{(\Delta \cdot k - \Delta \cdot q)} \left[ \frac{1}{D_k^2 D_q D_{kp} D_{kqp}} \right. \\ &\quad + \frac{1}{D_q D_{kp}^2 D_{kq} D_{kqp}} + \frac{1}{D_k D_q D_{kp}^2 D_{kq}} + \frac{1}{D_k D_q D_{kp} D_{kqp}^2} \\ &\quad \left. - \frac{1}{D_k^2 D_{kp} D_{kq} D_{kqp}} - \frac{1}{D_k D_{kp}^2 D_{kq} D_{kqp}} \right]. \end{aligned} \quad (2.24)$$

As  $p^2 = 0$  the last two terms in (B.24) are equal to zero.

Finally we apply the method of partial integration to graph  $2f$ . The corresponding integral becomes

$$L^{(m)} = \int \frac{d^n q}{(2\pi)^n} \int \frac{d^n k}{(2\pi)^n} \frac{(\Delta \cdot k)^m - (\Delta \cdot q)^m}{(\Delta \cdot k - \Delta \cdot q)} \frac{1}{D_k D_q D_{kp} D_{qp} D_{kq}}, \quad (2.25)$$

with  $m_1^2 = m_2^2 = m_3^2 = m_4^2 = m^2$  and  $m_5^2 = 0$ .  $L^{(m)}$  can be split in the same way as done for  $K^{(m)}$  in (B.20). However because of the symmetry in  $k \leftrightarrow q$  one can simplify the calculation. Here we have

$$L^{(m)} = 2L_1^{(m)} = 2 \int \frac{d^n q}{(2\pi)^n} \int \frac{d^n k}{(2\pi)^n} \frac{(\Delta \cdot k)^m}{(\Delta \cdot k - \Delta \cdot q)} \frac{1}{D_k D_q D_{kp} D_{qp} D_{kq}}. \quad (2.26)$$

Differentiating the integrand with respect to  $q$  analogous to (B.13) we obtain

$$L_1^{(m)} = \frac{1}{n-5} \int \frac{d^n q}{(2\pi)^n} \int \frac{d^n k}{(2\pi)^n} \frac{(\Delta \cdot k)^m}{(\Delta \cdot k - \Delta \cdot q)} \left[ \frac{1}{D_k D_q^2 D_{kp} D_{qp}} + \frac{1}{D_k D_q D_{kp} D_{qp}^2} - \frac{1}{D_q^2 D_{kp} D_{qp} D_{kq}} - \frac{1}{D_k D_q D_{qp}^2 D_{kq}} \right]. \quad (2.27)$$

## Appendix C

Here we present the unrenormalized operator matrix elements  $\hat{A}_{ij}^{(2)}$  whose general structure expressed in renormalization group coefficients was derived in section 3. After having carried out mass renormalization the two-loop OME in fig. 2 is given by the following expression ( see also (3.22) )

$$\begin{aligned}
\hat{A}_{Qg}^{(2)}\left(\frac{\mu^2}{m^2}, \epsilon\right) &= S_\epsilon^2\left(\frac{m^2}{\mu^2}\right)^\epsilon \left[ \frac{1}{\epsilon^2} \left\{ C_F T_f [(32 - 64z + 64z^2) \ln(1 - z) \right. \right. \\
&\quad \left. \left. - (16 - 32z + 64z^2) \ln z - (8 - 32z)] \right. \right. \\
&\quad \left. \left. + C_A T_f \left[ - (32 - 64z + 64z^2) \ln(1 - z) - (32 + 128z) \ln z - \frac{64}{3z} \right. \right. \right. \\
&\quad \left. \left. - 16 - 128z + \frac{496}{3} z^2 \right] \right\} \\
&\quad + \frac{1}{\epsilon} \left\{ C_F T_f \left[ (8 - 16z + 16z^2) [2 \ln z \ln(1 - z) - \ln^2(1 - z) + 2\zeta(2)] \right. \right. \\
&\quad \left. \left. - (4 - 8z + 16z^2) \ln^2 z - 32z(1 - z) \ln(1 - z) \right. \right. \\
&\quad \left. \left. - (12 - 16z + 32z^2) \ln z - 56 + 116z - 80z^2 \right] \right. \\
&\quad \left. + C_A T_f \left[ (16 + 32z + 32z^2) [\text{Li}_2(-z) + \ln z \ln(1 + z)] \right. \right. \\
&\quad \left. \left. + (8 - 16z + 16z^2) \ln^2(1 - z) + (8 + 16z) \ln^2 z \right. \right. \\
&\quad \left. \left. + 32z\zeta(2) + 32z(1 - z) \ln(1 - z) - \left( 8 + 64z + \frac{352}{3} z^2 \right) \ln z \right. \right. \\
&\quad \left. \left. - \frac{160}{9z} + 16 - 200z + \frac{1744}{9} z^2 \right] \right\} + a_{Qg}^{(2)}(z) \\
&\quad + \sum_{H=c,b,t} S_\epsilon^2\left(\frac{m_H^2}{\mu^2}\right)^{\epsilon/2} \left(\frac{m^2}{\mu^2}\right)^{\epsilon/2} \left[ \frac{1}{\epsilon^2} T_f^2 \left( -\frac{64}{3} + \frac{128}{3} z - \frac{128}{3} z^2 \right) \right. \\
&\quad \left. \times \left( 1 + \frac{\epsilon^2}{4} \zeta(2) \right) \right], \tag{3.1}
\end{aligned}$$

with

$$\begin{aligned}
a_{Qg}^{(2)}(z) &= C_F T_f \left\{ (1 - 2z + 2z^2) [8\zeta(3) + 8\zeta(2) \ln(1 - z) + \frac{4}{3} \ln^3(1 - z) \right. \\
&\quad \left. - 8 \ln(1 - z) \text{Li}_2(1 - z) + 4\zeta(2) \ln z - 4 \ln z \ln^2(1 - z) \right. \\
&\quad \left. + \frac{2}{3} \ln^3 z - 8 \ln z \text{Li}_2(1 - z) + 8 \text{Li}_3(1 - z) - 24 \text{S}_{1,2}(1 - z) \right\}
\end{aligned}$$

$$\begin{aligned}
& +z^2 \left[ -24\zeta(2) \ln z + \frac{4}{3} \ln^3 z + 16 \ln z \text{Li}_2(1-z) + 32\text{S}_{1,2}(1-z) \right] \\
& - (4 + 96z - 64z^2) \text{Li}_2(1-z) - (6 - 56z + 40z^2) \zeta(2) \\
& - (8 + 48z - 24z^2) \ln z \ln(1-z) + (4 + 8z - 12z^2) \ln^2(1-z) \\
& - (1 + 12z - 20z^2) \ln^2 z - (52z - 48z^2) \ln(1-z) \\
& - (16 + 18z + 48z^2) \ln z + 26 - 82z + 80z^2 \} \\
& + C_A T_f \left\{ (1 - 2z + 2z^2) [-8\zeta(2) \ln(1-z) - \frac{4}{3} \ln^3(1-z) \right. \\
& + 8 \ln(1-z) \text{Li}_2(1-z) - 8 \text{Li}_3(1-z)] + (1 + 2z + 2z^2) \\
& \times [-8\zeta(2) \ln(1+z) - 16 \ln(1+z) \text{Li}_2(-z) - 8 \ln z \ln^2(1+z) \\
& + 4 \ln^2 z \ln(1+z) + 8 \ln z \text{Li}_2(-z) - 8 \text{Li}_3(-z) - 16 \text{S}_{1,2}(-z)] \\
& + (16 + 64z) [2\text{S}_{1,2}(1-z) + \ln z \text{Li}_2(1-z)] - \left( \frac{4}{3} + \frac{8}{3} z \right) \ln^3 z \\
& + (8 - 32z + 16z^2) \zeta(3) - (24 + 96z) \zeta(2) \ln z + (16 + 16z^2) \\
& \times [\text{Li}_2(-z) + \ln z \ln(1+z)] + \left( \frac{32}{3z} + 12 + 64z - \frac{272}{3} z^2 \right) \text{Li}_2(1-z) \\
& - \left( 16 + 80z - 128z^2 + \frac{16}{z} \right) \zeta(2) - 4z^2 \ln z \ln(1-z) \\
& - (2 + 8z - 10z^2) \ln^2(1-z) + \left( 2 + 8z + \frac{46}{3} z^2 \right) \ln^2 z \\
& + (4 + 16z - 16z^2) \ln(1-z) - \left( \frac{56}{3} + \frac{172}{3} z + \frac{1600}{9} z^2 \right) \ln z \\
& \left. - \frac{448}{27z} - \frac{4}{3} - \frac{628}{3} z + \frac{6352}{27} z^2 \right\}. \tag{3.2}
\end{aligned}$$

The unrenormalized OME corresponding to fig.3 ( see (3.29) ) is given by

$$\begin{aligned}
\hat{A}_{Qq}^{\text{PS},(2)} \left( \frac{\mu^2}{m^2}, \epsilon \right) &= S_\epsilon^2 \left( \frac{m^2}{\mu^2} \right)^\epsilon C_F T_f \left\{ \frac{1}{\epsilon^2} \left( -32(1+z) \ln z - \frac{64}{3z} - 16 \right. \right. \\
& + 16z + \frac{64}{3} z^2 \left. \right) + \frac{1}{\epsilon} \left( 8(1+z) \ln^2 z - \left( 8 + 40z + \frac{64}{3} z^2 \right) \ln z - \frac{160}{9z} \right. \\
& \left. \left. + 16 - 48z + \frac{448}{9} z^2 \right) + a_{Qq}^{\text{PS},(2)}(z) \right\}, \tag{3.3}
\end{aligned}$$

with

$$a_{Qq}^{\text{PS},(2)}(z) = \left[ (1+z) \left( 32\text{S}_{1,2}(1-z) + 16 \ln z \text{Li}_2(1-z) - 24\zeta(2) \ln z \right. \right.$$

$$\begin{aligned}
& -\frac{4}{3} \ln^3 z) + \left(\frac{32}{3z} + 8 - 8z - \frac{32}{3}z^2\right) \text{Li}_2(1-z) \\
& + \left(-\frac{16}{z} - 12 + 12z + 16z^2\right) \zeta(2) + \left(2 + 10z + \frac{16}{3}z^2\right) \ln^2 z \\
& - \left(\frac{56}{3} + \frac{88}{3}z + \frac{448}{9}z^2\right) \ln z - \frac{448}{27z} - \frac{4}{3} - \frac{124}{3}z + \frac{1600}{27}z^2 \Big]. \quad (3.4)
\end{aligned}$$

The unrenormalized OME corresponding to fig.4 is (see (3.33))

$$\begin{aligned}
\hat{A}_{qq,Q}^{\text{NS},(2)}\left(\frac{\mu^2}{m^2}, \epsilon\right) &= S_\epsilon^2\left(\frac{m^2}{\mu^2}\right)^\epsilon C_{FTf} \left\{ \frac{1}{\epsilon^2} \left[ \frac{32}{3} \left(\frac{1}{1-z}\right)_+ - \frac{16}{3} - \frac{16}{3}z + 8\delta(1-z) \right] \right. \\
&+ \frac{1}{\epsilon} \left[ \frac{80}{9} \left(\frac{1}{1-z}\right)_+ + \frac{8}{3} \frac{1+z^2}{1-z} \ln z + \frac{8}{9} - \frac{88}{9}z + \delta(1-z) \left(\frac{16}{3}\zeta(2) + \frac{2}{3}\right) \right] \\
&\left. + a_{qq,Q}^{\text{NS},(2)}(z) \right\}, \quad (3.5)
\end{aligned}$$

with

$$\begin{aligned}
a_{qq,Q}^{\text{NS},(2)}(z) &= \left(\frac{8}{3} \left(\frac{1}{1-z}\right)_+ - \frac{4}{3} - \frac{4}{3}z\right) \zeta(2) + \frac{1+z^2}{1-z} \left(\frac{2}{3} \ln^2 z + \frac{20}{9} \ln z\right) \\
&+ \frac{8}{3}(1-z) \ln z + \frac{224}{27} \left(\frac{1}{1-z}\right)_+ + \frac{44}{27} - \frac{268}{27}z \\
&+ \delta(1-z) \left(-\frac{8}{3}\zeta(3) + \frac{58}{9}\zeta(2) + \frac{73}{18}\right). \quad (3.6)
\end{aligned}$$

Here the term  $1/(1-z)_+$  has to be defined in the distribution sense

$$\int_0^1 dz \left(\frac{1}{1-z}\right)_+ f(z) = \int_0^1 dz \frac{1}{1-z} [f(z) - f(1)]. \quad (3.7)$$

Notice that as long as  $z < Q^2/(Q^2+4m^2)$  with  $m^2 \neq 0$  the terms proportional to  $\delta(1-z)$  do not contribute and the subscript  $+$  in  $(1/(1-z))_+$  can be dropped. We will comment on this in Appendix D after having predicted the asymptotic expression for  $L_{2,q}^{\text{NS},(2)}(z, Q^2, m^2)$ . The OME's which emerge from the calculation of graphs 1-4 usually appear in the Mellin transformed representation

$$A_{ij}^{(m)} = \frac{1}{2} [1 + (-1)^m] \int_0^1 dz z^{m-1} A_{ij}(z). \quad (3.8)$$

This implies that the anomalous dimensions  $\gamma_{ij}^{(m)}$  correspond to the physical operators listed in eqs.(2.24)-(2.26) only for even  $m$ .

## Appendix D

In this appendix we present the heavy quark coefficient functions  $H_{i,j}^{(2)}$  and  $L_{i,j}^{(2)}$  ( $i = L, 2; j = q, g$ ) in the asymptotic limit  $Q^2 \gg m^2$ . Starting with process (2.11) the heavy quark coefficient functions read ( see (4.6), (4.7) )

$$H_{L,g}^{(1)}(z, Q^2, m^2) = T_f[16z(1-z)], \quad (4.1)$$

$$H_{2,g}^{(1)}(z, Q^2, m^2) = T_f[(4 - 8z + 8z^2) \left( \ln \frac{Q^2}{m^2} + \ln(1-z) - \ln z \right) - 4 + 32z - 32z^2]. \quad (4.2)$$

In next-to-leading order the coefficient functions given by process (2.12) and expressions (4.14), (4.15) read

$$\begin{aligned} H_{L,g}^{(2)}(z, Q^2, m^2) = & \left[ C_F T_f \{ 32z \ln z + 16 + 16z - 32z^2 \} \right. \\ & + C_A T_f \left\{ 64z(1-z) \ln(1-z) - 128z \ln z + \frac{32}{3z} - 32 \right. \\ & \left. \left. - 160z + \frac{544}{3} z^2 \right\} \right] \ln \frac{Q^2}{m^2} \\ & + C_A T_f \left\{ 64z(1-z) \ln(1-z) - 128z \ln z + \frac{32}{3z} - 32 \right. \\ & \left. \left. - 160z + \frac{544}{3} z^2 \right\} \ln \frac{m^2}{\mu^2} \right. \\ & + C_F T_f \left\{ \left( \frac{64}{15z^2} - \frac{64}{3}z + \frac{128}{5}z^3 \right) [\text{Li}_2(-z) + \ln z \ln(1+z)] \right. \\ & + 32z [\text{Li}_2(1-z) + \ln z \ln(1-z)] - \left( \frac{64}{3}z - \frac{128}{5}z^3 \right) \zeta(2) \\ & - \left( \frac{64}{3}z + \frac{64}{5}z^3 \right) \ln^2 z + (16 + 48z - 64z^2) \ln(1-z) \\ & + \left( -\frac{64}{15z} - \frac{208}{15} - \frac{416}{5}z + \frac{192}{5}z^2 \right) \ln z + \frac{64}{15z} - \frac{256}{15} - \frac{608}{5}z + \frac{672}{5}z^2 \left. \right\} \\ & + C_A T_f \left\{ (64z + 64z^2) [\text{Li}_2(-z) + \ln z \ln(1+z)] - 128z \text{Li}_2(1-z) \right. \\ & + 64z^2 \zeta(2) - (192z - 64z^2) \ln z \ln(1-z) + (32z - 32z^2) \ln^2(1-z) \\ & + 96z \ln^2 z + \left( \frac{32}{3z} - 32 - 288z + \frac{928}{3}z^2 \right) \ln(1-z) \\ & \left. + (32 + 256z - 416z^2) \ln z - \frac{32}{9z} + \frac{32}{3} + \frac{544}{3}z - \frac{1696}{9}z^2 \right\}, \quad (4.3) \end{aligned}$$



$$\begin{aligned}
H_{2,g}^{(2)}(z, Q^2, m^2) = & \left[ C_F T_f \{ (8 - 16z + 16z^2) \ln(1 - z) \right. \\
& - (4 - 8z + 16z^2) \ln z - 2 + 8z \} \\
& + C_A T_f \{ (8 - 16z + 16z^2) \ln(1 - z) + (8 + 32z) \ln z + \frac{16}{3z} \\
& + 4 + 32z - \frac{124}{3} z^2 \} \left. \right] \ln^2 \frac{Q^2}{m^2} \\
& + \left[ C_F T_f \{ (8 - 16z) \text{Li}_2(1 - z) - (32 - 64z + 64z^2) \zeta(2) \right. \\
& - (24 - 48z + 64z^2) \ln z \ln(1 - z) + (16 - 32z + 32z^2) \ln^2(1 - z) \\
& + (8 - 16z + 32z^2) \ln^2 z - (28 - 96z + 80z^2) \ln(1 - z) \\
& + (8 - 48z + 80z^2) \ln z + 36 - 68z + 16z^2 \} \\
& + C_A T_f \{ -(16 + 32z + 32z^2) [\text{Li}_2(-z) + \ln z \ln(1 + z)] \\
& + (16 + 64z) \text{Li}_2(1 - z) - (16 + 32z^2) \zeta(2) \\
& + (96z - 32z^2) \ln z \ln(1 - z) + (8 - 16z + 16z^2) \ln^2(1 - z) \\
& - (16 + 48z) \ln^2 z + \left( \frac{32}{3z} - 8 + 160z - \frac{536}{3} z^2 \right) \ln(1 - z) \\
& \left. - (192z - 200z^2) \ln z + \frac{208}{9z} - \frac{220}{3} - \frac{368}{3} z + \frac{1628}{9} z^2 \right\} \ln \frac{Q^2}{m^2} \\
& + C_A T_f \left[ \{ (16 - 32z + 32z^2) \ln(1 - z) + (16 + 64z) \ln z + \frac{32}{3z} + 8 \right. \\
& + 64z - \frac{248}{3} z^2 \} \ln \frac{Q^2}{m^2} \\
& + (16 + 64z) \text{Li}_2(1 - z) - (16 - 32z + 32z^2) \zeta(2) \\
& + (96z - 32z^2) \ln z \ln(1 - z) + (16 - 32z + 32z^2) \ln^2(1 - z) \\
& - (8 + 32z) \ln^2 z + \left( \frac{32}{3z} - 8 + 192z - \frac{632}{3} z^2 \right) \ln(1 - z) \\
& \left. - \left( 8 + 256z - \frac{248}{3} z^2 \right) \ln z + \frac{16}{3z} - \frac{172}{3} - \frac{968}{3} z + \frac{1124}{3} z^2 \right] \ln \frac{m^2}{\mu^2} \\
& + C_F T_f \left[ 16(1 + z)^2 \left( -4\text{S}_{1,2}(-z) - 4 \ln(1 + z) \text{Li}_2(-z) \right. \right. \\
& \left. \left. - 2\zeta(2) \ln(1 + z) - 2 \ln z \ln^2(1 + z) + \ln^2 z \ln(1 + z) - \frac{3}{2} \text{Li}_2(1 - z) \right) \right. \\
& \left. + 8(1 - z)^2 \left( -4\text{S}_{1,2}(1 - z) - 3\text{Li}_3(1 - z) + 12\text{Li}_3(-z) + \ln^3(1 - z) \right. \right. \\
& \left. \left. - \frac{5}{2} \ln z \ln^2(1 - z) + 2 \ln^2 z \ln(1 - z) + \ln(1 - z) \text{Li}_2(1 - z) \right) \right]
\end{aligned}$$

$$\begin{aligned}
& -4 \ln z \operatorname{Li}_2(-z) + 4\zeta(2) \ln z - \frac{1}{3} \ln^3 z + 3 \ln z \ln(1-z) \\
& + 8z^2 \left( 4S_{1,2}(1-z) - \operatorname{Li}_3(1-z) + \ln^3(1-z) \right) \\
& - \frac{7}{2} \ln z \ln^2(1-z) + 4 \ln^2 z \ln(1-z) - \ln(1-z) \operatorname{Li}_2(1-z) \\
& - 4\zeta(2) \ln(1-z) + 4 \ln z \operatorname{Li}_2(1-z) + 4\zeta(2) \ln z - \ln^3 z + 11 \operatorname{Li}_2(1-z) \\
& + 128z \operatorname{Li}_3(-z) + (112 - 96z + 192z^2) \zeta(3) - (112z - 144z^2) \ln z \ln(1-z) \\
& + \left( \frac{16}{15z^2} + 96 + \frac{128}{3}z + \frac{192}{5}z^3 \right) [\operatorname{Li}_2(-z) + \ln z \ln(1+z)] \\
& + \left( 48 - \frac{208}{3}z + 104z^2 + \frac{192}{5}z^3 \right) \zeta(2) - (22 - 88z + 84z^2) \ln^2(1-z) \\
& - \left( 4 - \frac{8}{3}z + 52z^2 + \frac{96}{5}z^3 \right) \ln^2 z + (28 - 132z + 96z^2) \ln(1-z) \\
& - \left( \frac{16}{15z} + \frac{712}{15} - \frac{136}{5}z + \frac{672}{5}z^2 \right) \ln z + \frac{16}{15z} - \frac{904}{15} + \frac{68}{5}z + \frac{328}{5}z^2 \\
& + C_A T_f \left[ 16(1+2z+2z^2) \left( \operatorname{Li}_3\left(\frac{1-z}{1+z}\right) - \operatorname{Li}_3\left(-\frac{1-z}{1+z}\right) \right) \right. \\
& \left. - \ln z \ln(1-z) \ln(1+z) - \ln(1-z) \operatorname{Li}_2(-z) \right. \\
& \left. + \frac{3}{4} \ln^2 z \ln(1+z) + \frac{3}{2} \ln z \operatorname{Li}_2(-z) \right) \\
& + 8(1+2z) [5S_{1,2}(1-z) + 2S_{1,2}(-z) - 3\operatorname{Li}_3(-z) + \ln z \ln^2(1+z) \\
& + 2 \ln(1+z) \operatorname{Li}_2(-z) + \zeta(2) \ln(1+z)] \\
& + 32z [2S_{1,2}(1-z) + \ln z \operatorname{Li}_2(1-z)] \\
& - (16 + 128z) \operatorname{Li}_3(1-z) + 8z^2 [\ln^2 z \ln(1+z) \\
& - 2 \ln z \operatorname{Li}_2(-z)] + (48z - 16z^2) \ln z \ln^2(1-z) \\
& - (8 + 64z - 16z^2) \ln^2 z \ln(1-z) + (16 + 64z) \ln(1-z) \operatorname{Li}_2(1-z) \\
& - (40 - 48z + 64z^2) \zeta(2) \ln(1-z) + \left( \frac{16}{3} + 16z \right) \ln^3 z \\
& - (16 + 160z - 32z^2) \zeta(2) \ln z - (12 + 56z + 8z^2) \zeta(3) \\
& - \left( \frac{32}{3z} + 48 - 16z - \frac{208}{3}z^2 \right) [\operatorname{Li}_2(-z) + \ln z \ln(1+z)] + \left( \frac{64}{3z} + 20 \right. \\
& \left. - 64z + \frac{80}{3}z^2 \right) \operatorname{Li}_2(1-z) - \left( \frac{32}{z} + 4 + 208z - \frac{796}{3}z^2 \right) \zeta(2) \\
& + (16 - 288z + 292z^2) \ln z \ln(1-z) + \left( \frac{16}{3z} - 6 + 64z - \frac{214}{3}z^2 \right) \ln^2(1-z)
\end{aligned}$$

$$\begin{aligned}
& +(184z - 114z^2) \ln^2 z + \left( \frac{208}{9z} - \frac{112}{3} - \frac{860}{3}z + \frac{2996}{9}z^2 \right) \ln(1-z) \\
& + \left( \frac{292}{3} + 332z - \frac{5780}{9}z^2 \right) \ln z + \frac{80}{9z} + \frac{466}{9} + \frac{260}{9}z - \frac{878}{9}z^2 \Big]. \quad (4.4)
\end{aligned}$$

The coefficient function corresponding to the Bethe-Heitler process (2.13) reads (see (4.20), (4.21))

$$\begin{aligned}
H_{L,q}^{(2)}(z, Q^2, m^2) &= C_F T_f \left[ \left\{ -32z \ln z + \frac{32}{3z} - 32 + \frac{64}{3}z^2 \right\} \right. \\
&\quad \times \left\{ \ln \frac{Q^2}{m^2} + \ln \frac{m^2}{\mu^2} \right\} - 32z [\text{Li}_2(1-z) + \ln z \ln(1-z) - \ln^2 z] \\
&\quad + \left( \frac{32}{3z} - 32 + \frac{64}{3}z^2 \right) \ln(1-z) + (32 - 32z - 64z^2) \ln z \\
&\quad \left. - \frac{32}{9z} + \frac{32}{3} - \frac{128}{3}z + \frac{320}{9}z^2 \right], \quad (4.5)
\end{aligned}$$

$$\begin{aligned}
H_{2,q}^{(2)}(z, Q^2, m^2) &= C_F T_f \left[ \left\{ 8(1+z) \ln z + \frac{16}{3z} + 4 - 4z - \frac{16}{3}z^2 \right\} \ln^2 \frac{Q^2}{m^2} \right. \\
&\quad + \left\{ [16(1+z) \ln z + \frac{32}{3z} + 8 - 8z - \frac{32}{3}z^2] \ln \frac{Q^2}{m^2} \right. \\
&\quad + 8(1+z) [2\text{Li}_2(1-z) + 2 \ln z \ln(1-z) - \ln^2 z] \\
&\quad + \left( \frac{32}{3z} + 8 - 8z - \frac{32}{3}z^2 \right) \ln(1-z) \\
&\quad - \left( 8 + 40z - \frac{32}{3}z^2 \right) \ln z + \frac{16}{3z} - \frac{160}{3} + \frac{16}{3}z + \frac{128}{3}z^2 \Big\} \ln \frac{m^2}{\mu^2} \\
&\quad + \{ 16(1+z) [\text{Li}_2(1-z) + \ln z \ln(1-z) - \ln^2 z] \\
&\quad + \left( \frac{32}{3z} + 8 - 8z - \frac{32}{3}z^2 \right) \ln(1-z) + 32z^2 \ln z + \frac{208}{9z} - \frac{208}{3} \\
&\quad + \frac{160}{3}z - \frac{64}{9}z^2 \Big\} \ln \frac{Q^2}{m^2} \\
&\quad + (1+z) \left( 32\text{S}_{1,2}(1-z) - 16\text{Li}_3(1-z) + 8 \ln z \ln^2(1-z) \right. \\
&\quad - 16 \ln^2 z \ln(1-z) + 16 \ln(1-z) \text{Li}_2(1-z) - 32\zeta(2) \ln z + \frac{16}{3} \ln^3 z \Big) \\
&\quad - \left( \frac{32}{3z} + 32 + 32z + \frac{32}{3}z^2 \right) [\text{Li}_2(-z) + \ln z \ln(1+z)] \\
&\quad \left. + \left( \frac{64}{3z} + 16 - 16z + \frac{32}{3}z^2 \right) \text{Li}_2(1-z) - \left( \frac{32}{z} + 16 + 16z - \frac{64}{3}z^2 \right) \zeta(2) \right]
\end{aligned}$$

$$\begin{aligned}
& +32z^2 \ln z \ln(1-z) + \left(\frac{16}{3z} + 4 - 4z - \frac{16}{3}z^2\right) \ln^2(1-z) \\
& + (40z - 16z^2) \ln^2 z + \left(\frac{208}{9z} - \frac{208}{3} + \frac{160}{3}z - \frac{64}{9}z^2\right) \ln(1-z) \\
& + \left(\frac{280}{3} - 88z - \frac{704}{9}z^2\right) \ln z \\
& + \left[\frac{80}{9z} + \frac{304}{9} - \frac{1216}{9}z + \frac{832}{9}z^2\right]. \tag{4.6}
\end{aligned}$$

Finally we present the coefficient functions corresponding to the Compton process (2.13). They are given by eqs. (4.28), (4.29) which become equal to

$$\begin{aligned}
L_{L,q}^{\text{NS},(2)}(z, Q^2, m^2) &= C_F T_f \left[ \frac{16}{3} z \left( \ln \frac{Q^2}{m^2} + \ln(1-z) - 2 \ln z \right) \right. \\
&\quad \left. + \frac{16}{3} - \frac{400}{18} z \right], \tag{4.7}
\end{aligned}$$

$$\begin{aligned}
L_{2,q}^{\text{NS},(2)}(z, Q^2, m^2) &= C_F T_f \left[ \frac{4}{3} \left( \frac{1+z^2}{1-z} \right) \ln^2 \frac{Q^2}{m^2} + \left\{ \frac{1+z^2}{1-z} \left( \frac{8}{3} \ln(1-z) \right. \right. \right. \\
&\quad \left. \left. - \frac{16}{3} \ln z - \frac{58}{9} \right) + \frac{2}{3} + \frac{26}{3} z \right\} \ln \frac{Q^2}{m^2} \\
&\quad + \left( \frac{1+z^2}{1-z} \right) \left( -\frac{8}{3} \text{Li}_2(1-z) - \frac{8}{3} \zeta(2) - \frac{16}{3} \ln z \ln(1-z) \right) \\
&\quad + \frac{4}{3} \ln^2(1-z) + 4 \ln^2 z - \frac{58}{9} \ln(1-z) + \frac{134}{9} \ln z + \frac{359}{27} \\
&\quad \left. + \left( \frac{2}{3} + \frac{26}{3} z \right) \ln(1-z) - \left( 2 + \frac{46}{3} z \right) \ln z + \frac{29}{9} - \frac{295}{9} z \right]. \tag{4.8}
\end{aligned}$$

In the above expressions one should bear in mind that the singularity at  $z = 1$  will never show up because of the kinematical constraint  $z < Q^2/(Q^2 + 4m^2)$ . However after convoluting  $L_{2,q}^{\text{NS}}$  by the parton densities the structure function  $F_2(z, Q^2, m^2)$  in (2.8) will diverge as  $\ln^3(Q^2/m^2)$  in the limit  $Q^2 \gg m^2$ . In the above limit the upper boundary in (2.8)  $z_{max} \rightarrow 1$  and the virtual gluon which decays into the heavy quark pair becomes soft. The soft gluon contribution which causes the cubic logarithm above has to be added to the two-loop virtual gluon corrections calculated in appendix A of [27]. The cubic logarithm is then cancelled. The final result will be that in (D.8) the

singular terms at  $z = 1$  have to be replaced by the distributions  $(\ln^k(1 - z))/(1 - z)_+$  defined by

$$\int_0^1 dz \left( \frac{\ln^k(1 - z)}{1 - z} \right)_+ f(z) = \int_0^1 dz \left( \frac{\ln^k(1 - z)}{1 - z} \right) (f(z) - f(1)), \quad (4.9)$$

and one has to add the following delta function contribution

$$\begin{aligned} L_{2,q}^{\text{NS},S+V,(2)}(z, Q^2, m^2) = C_F T_f \delta(1 - z) \left\{ 2 \ln^2 \frac{Q^2}{m^2} - \left[ \frac{32}{3} \zeta(2) + \frac{38}{3} \right] \ln \frac{Q^2}{m^2} \right. \\ \left. + \frac{268}{9} \zeta(2) + \frac{265}{9} \right\}. \end{aligned} \quad (4.10)$$

## References

- [1] I. Abt et al. (H1-collaboration), Nucl. Phys. **B407** (1993) 515.
- [2] M. Derrick et al. (ZEUS-collaboration), Z. Phys. **C65** (1995) 379.
- [3] E. Laenen, S. Riemersma, J. Smith and W. L. van Neerven, Nucl. Phys. **B392** (1993) 162.
- [4] S.J. Brodsky, P. Hoyer, A.H. Mueller, W.-K. Tang, Nucl. Phys. **B369** (1992) 519.  
R. Vogt and S.J. Brodsky, Nucl. Phys. **B438**, (1995) 261.
- [5] M. Glück, E. Reya and M. Stratmann, Nucl. Phys. **B422** (1994) 37.
- [6] J. C. Collins, F. Wilczek and A. Zee, Phys. Rev. **D18** (1978) 242.
- [7] J. C. Collins and W.-T. Tung, Nucl. Phys. **B278** (1986) 934.  
W.-K. Tung, Nucl. Phys. **B315** (1989) 378.
- [8] M. A. G. Aivazis, F. I. Olness and W.-T. Tung, Phys. Rev. **D50** (1995) 3085.  
M. A. G. Aivazis, J. C. Collins, F. I. Olness and W.-T. Tung, Phys. Rev. **D50** (1995) 3102.
- [9] F. I. Olness and S. T. Riemersma, Phys. Rev. **D51** (1995) 4746.
- [10] G. Kramer, B. Lampe and H. Spiesberger, DESY-95-201.
- [11] E. B. Zijlstra and W. L. van Neerven, Nucl. Phys. **B383** (1992) 525.
- [12] S. Riemersma, J. Smith and W. L. van Neerven, Phys. Lett. **B347** (1995) 43. Some errors in the computer code used in this reference and in [3] are corrected in B. W. Harris and J. Smith, Nucl. Phys. **B452** (1995) 109.
- [13] F. A. Berends, W. L. van Neerven and G. J. H. Burgers, Nucl. Phys. **B297** (1988) 429.
- [14] B. Humpert and W.L. van Neerven, Nucl. Phys. **B178** (1981) 498.
- [15] R. Mertig and W.L. van Neerven, NIKHEF-H/95-031,INLO-PUB-6/95.

- [16] V.N. Gribov and L.N. Lipatov, Sov. J. Nucl. Phys. **15** (1972) 438,675;  
G. Altarelli and G. Parisi, Nucl. Phys. **B126** (1977) 298.
- [17] E.G. Floratos, D.A. Ross and C.T. Sachrajda, Nucl. Phys. **B129** (1977)  
66, Erratum **B139** (1978) 545; *ibid.* **B152** (1979) 493.
- [18] A. Gonzales-Arroyo, C. Lopez and F.J. Yndurain, Nucl. Phys. **B153**  
(1979) 161.  
A. Gonzales-Arroyo and C. Lopez, Nucl. Phys. **B166** (1980) 429.
- [19] E.G. Floratos, C. Kounnas and R. Lacaze, Phys. Lett. **B98** (1981)  
89,285; Nucl. Phys. **B192** (1981) 417.
- [20] G. Curci, W. Furmanski and R. Petronzio, Nucl. Phys. **B175** (1980) 27.  
W. Furmanski and R. Petronzio, Phys. Lett. **B97** (1980) 437; Z. Phys.  
**C11** (1982) 293.
- [21] L. Lewin, "Polylogarithms and Associated Functions", North Holland,  
Amsterdam, 1983.  
R. Barbieri, J.A. Mignaco and E. Remiddi, Nuovo Cimento **11A** (1972)  
824.  
A. Devoto and D.W. Duke, Riv. Nuovo. Cimento Vol. 7,N. 6 (1984) 1.
- [22] J. A. M. Vermaseren, FORM2, published by Computer Algebra Nether-  
lands (CAN), Kruislaan 413, 1098 SJ Amsterdam, The Netherlands.
- [23] K.G. Chetyrkin and F.V. Tkachov, Nucl. Phys. **B192** (1981) 159.
- [24] A. Djouadi and P. Gambino, Phys. Rev. **D49** (1994) 3499.
- [25] E.B. Zijlstra , Ph.D. thesis , University of Leiden , 1993.
- [26] S. Catani, M. Ciafaloni and F. Hautmann, Phys. Lett. **B242** (1990)  
97, "Production of heavy flavours at high energies", Proceedings of the  
Workshop "Physics at HERA", Hamburg, Oct. 29-30, 1991, Eds. W  
Buchmüller and G. Ingelman, Vol.2, 690.
- [27] P.J. Rijken and W.L. van Neerven, Phys. Rev. **D52** (1995) 149.

## Figure Captions

- Fig. 1.** a,b : One-loop graphs contributing to the OME  $A_{Qg}^{(1)}$ .  
c : Heavy quark ( $m_H^2 > Q^2$ ) loop contribution to  $A_{gg}^{(1)}$ . The solid line indicates the heavy quark  $Q$ .
- Fig. 2.** Two-loop graphs contributing to the OME  $A_{Qg}^{(2)}$ . The solid line indicates the heavy quark  $Q$ . Diagrams  $s$  and  $t$  with the external ghosts (dashed line) are needed to cancel the unphysical polarizations which appear in the sum of (3.43). Graphs  $u$  and  $v$  contain the external gluon self energy with the heavy quark ( $m_H^2 > Q^2$ ) loop.
- Fig. 3.** Two-loop graphs contributing to the OME  $A_{Qq}^{\text{PS},(2)}$ . The solid line represents the heavy quark  $Q$  whereas the dashed line stands for the light quark  $q$ .
- Fig. 4.** Two-loop graphs contributing to the OME  $A_{qq}^{\text{NS},(2)}$ . The solid line represents the heavy quark  $Q$  whereas the dashed line stands for the light quark  $q$ .
- Fig. 5.**  $R_{L,g}^{(1)}$  plotted as a function of  $\xi$  for fixed  $z = 10^{-2}$  (solid line) and  $z = 10^{-4}$  (dashed line).
- Fig. 6.**  $R_{2,g}^{(1)}$  plotted as a function of  $\xi$  for fixed  $z = 10^{-2}$  (solid line) and  $z = 10^{-4}$  (dashed line).
- Fig. 7.**  $R_{L,q}^{(1)}$  plotted as a function of  $\xi$  for fixed  $z = 10^{-2}$  (solid line) and  $z = 10^{-4}$  (dashed line).
- Fig. 8.**  $R_{2,q}^{(1)}$  plotted as a function of  $\xi$  for fixed  $z = 10^{-2}$  (solid line) and  $z = 10^{-4}$  (dashed line).
- Fig. 9.**  $T_{L,q}^{(1)}$  plotted as a function of  $\xi$  for fixed  $z = 10^{-2}$  (solid line) and  $z = 10^{-4}$  (dashed line).
- Fig. 10.**  $T_{2,q}^{(1)}$  plotted as a function of  $\xi$  for fixed  $z = 10^{-2}$  (solid line) and  $z = 10^{-4}$  (dashed line).



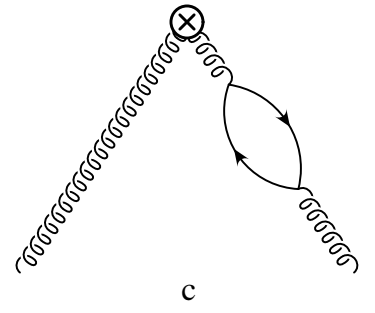
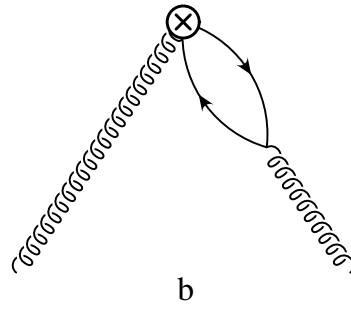
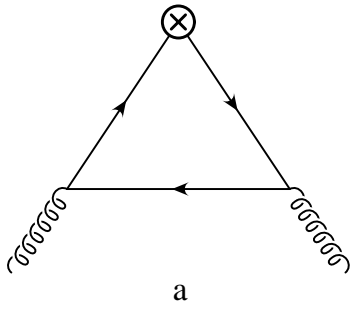


Fig. 1

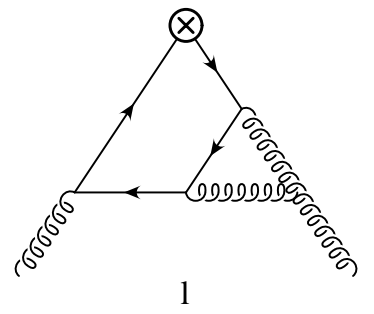
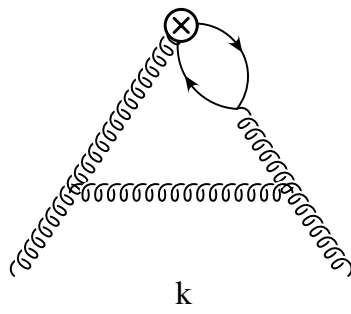
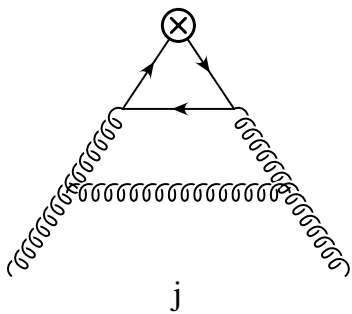
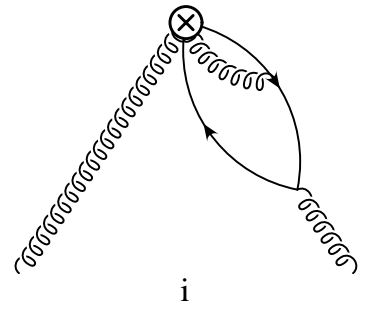
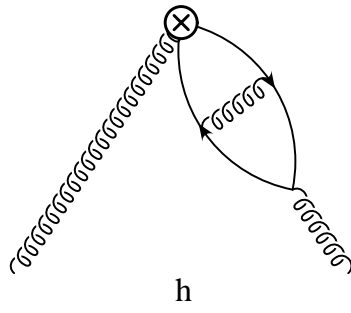
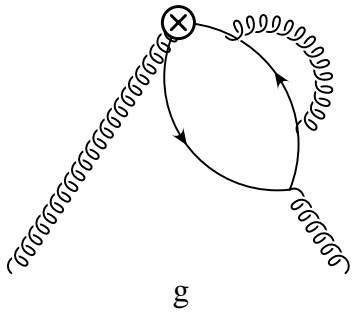
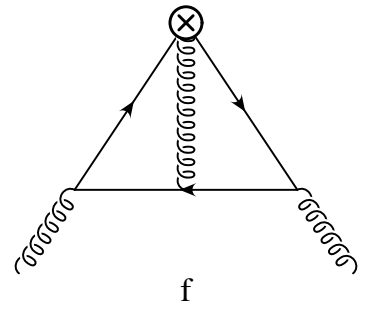
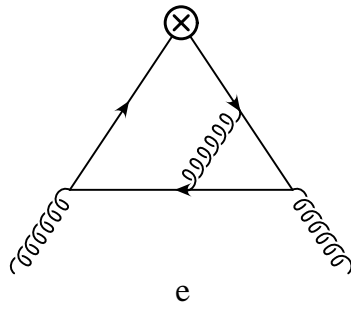
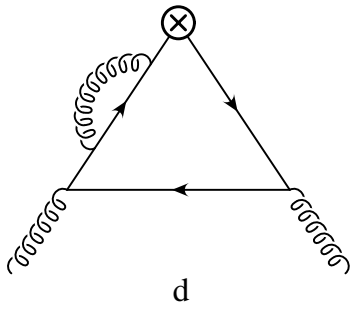
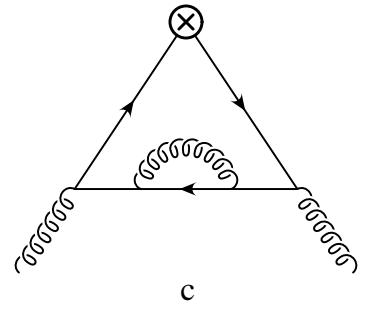
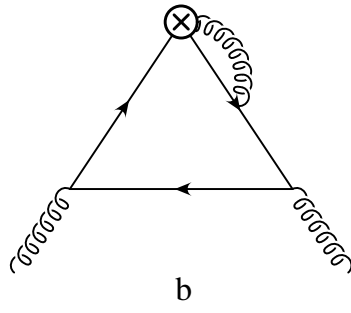
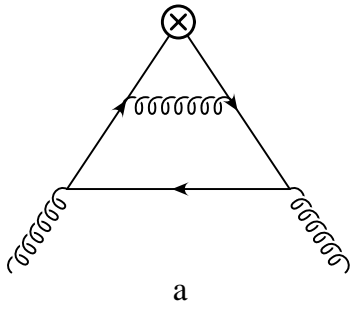


Fig. 2

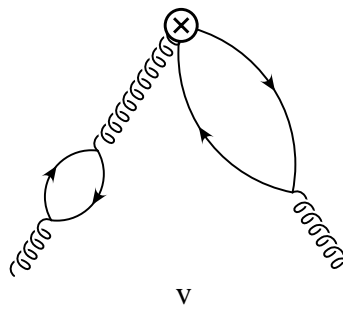
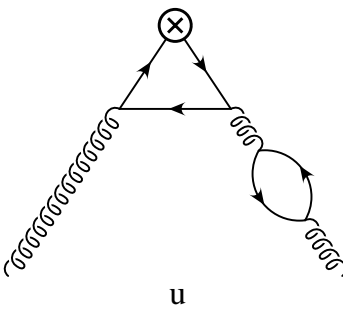
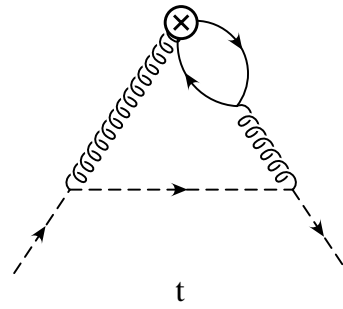
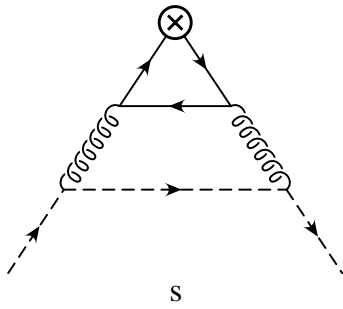
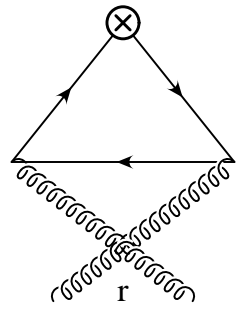
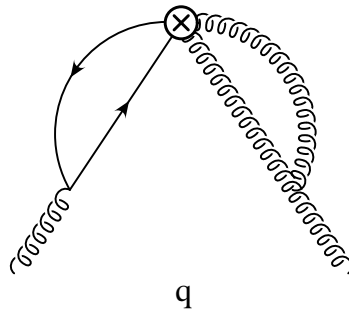
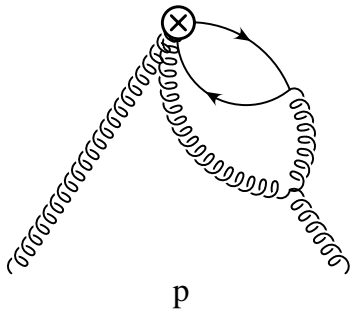
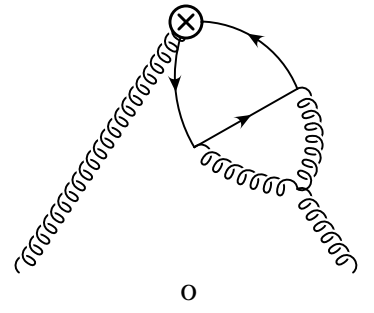
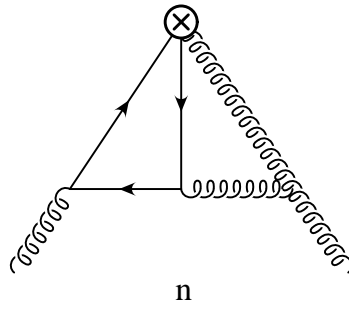
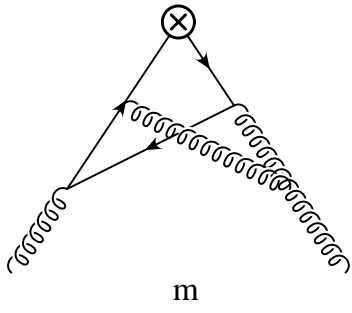


Fig. 2 (continued)

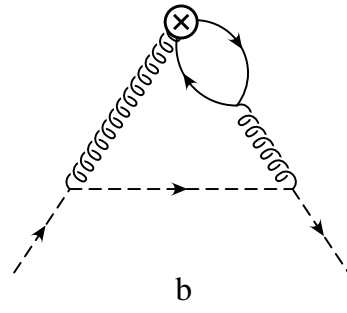
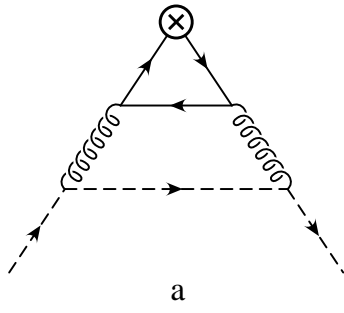


Fig. 3

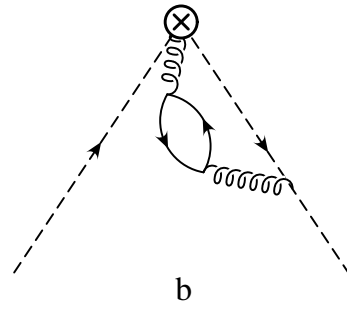
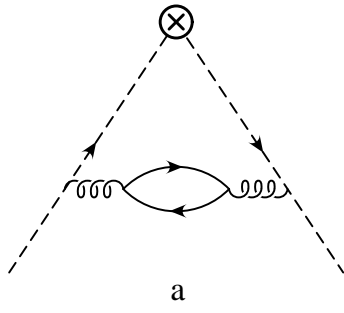


Fig. 4

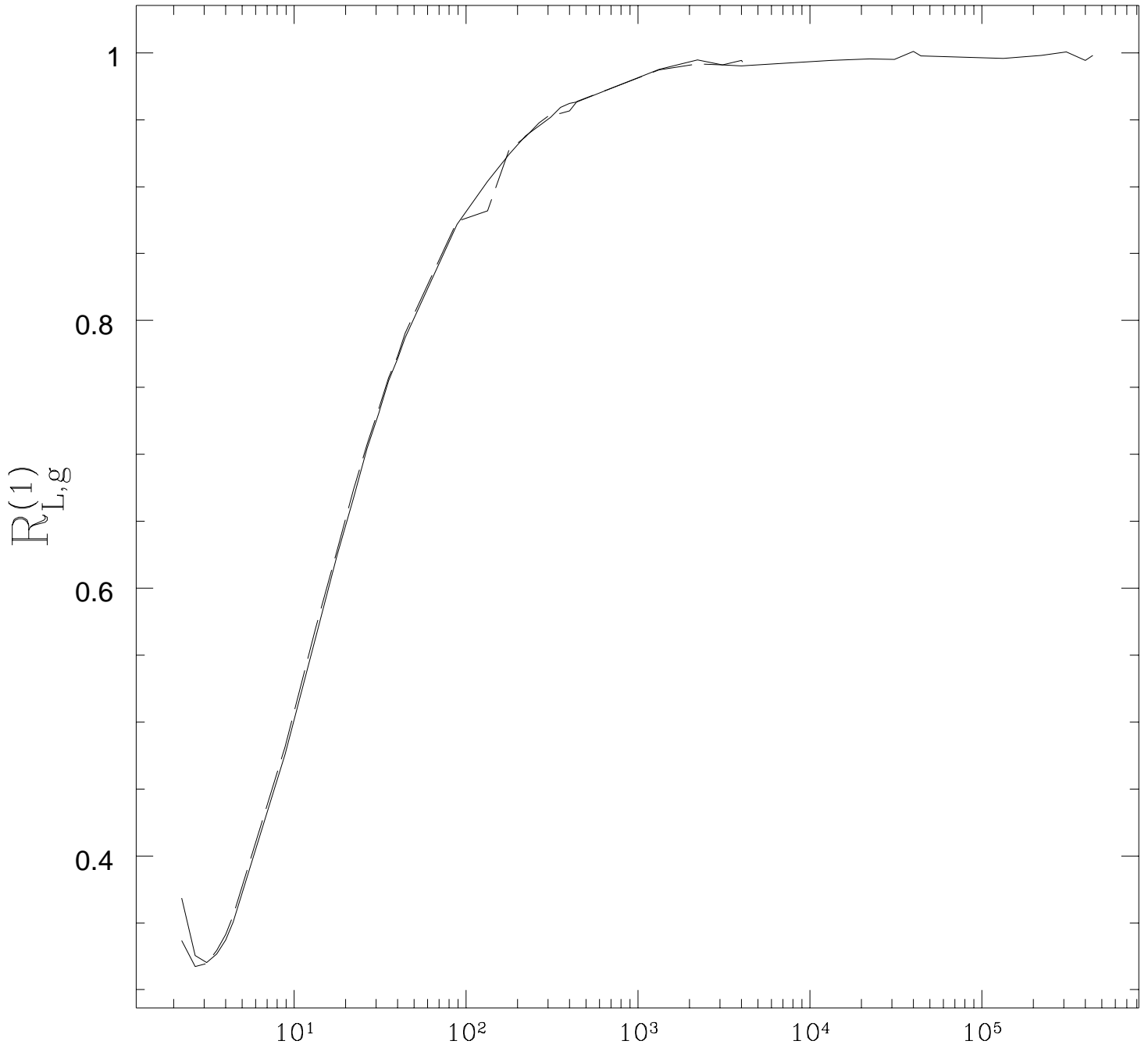


Fig. 5

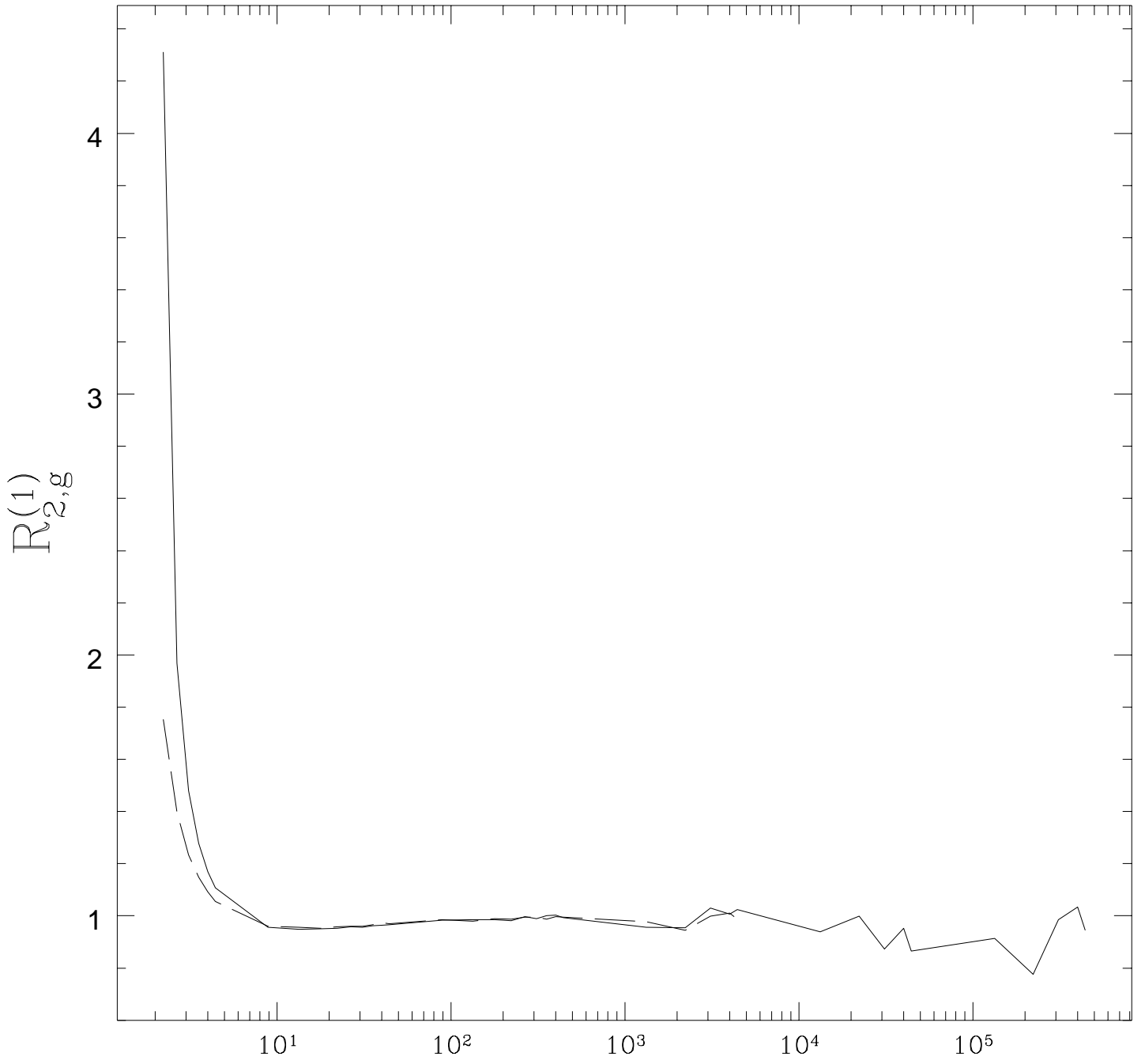


Fig. 6

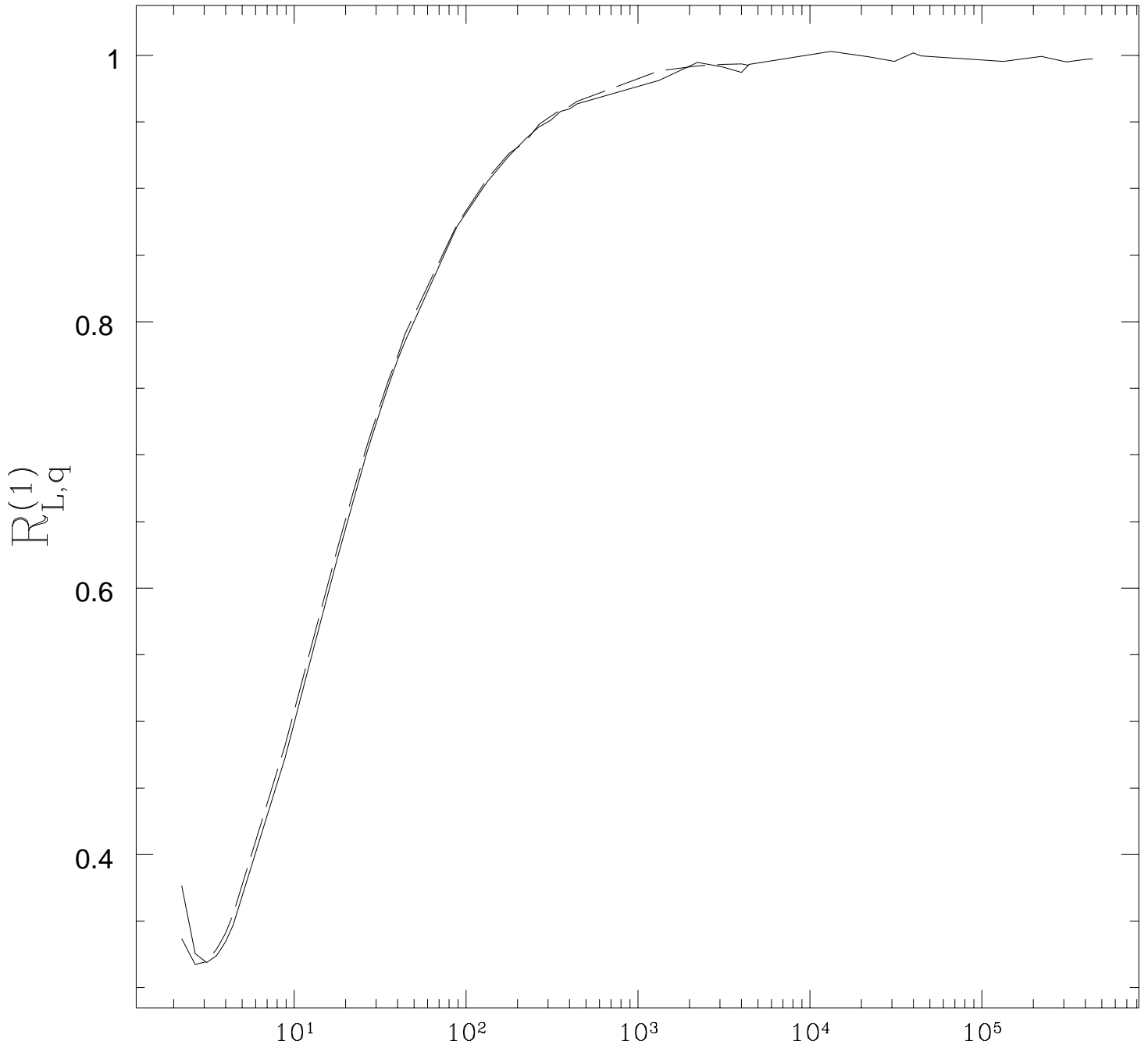


Fig. 7



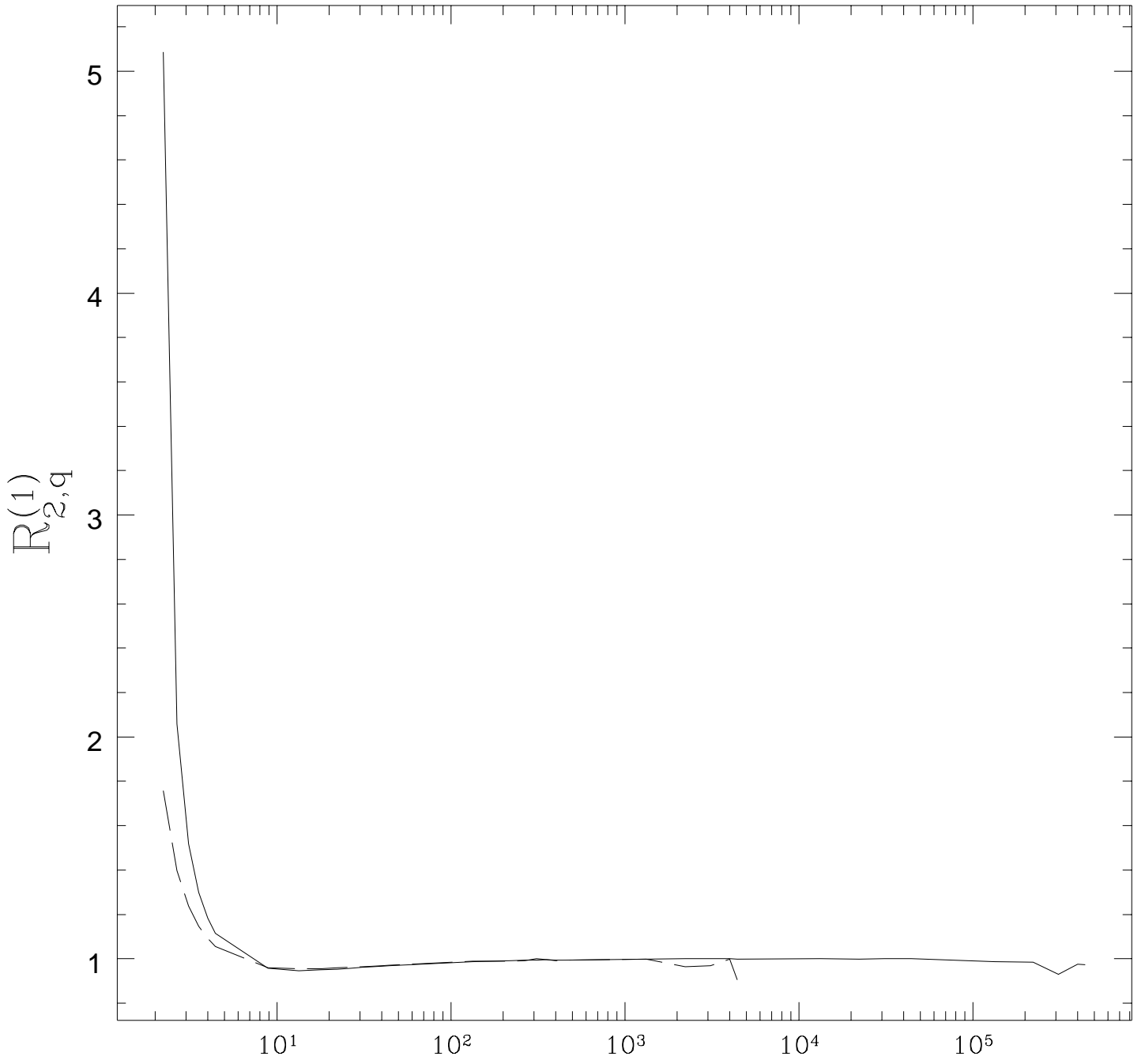


Fig. 8

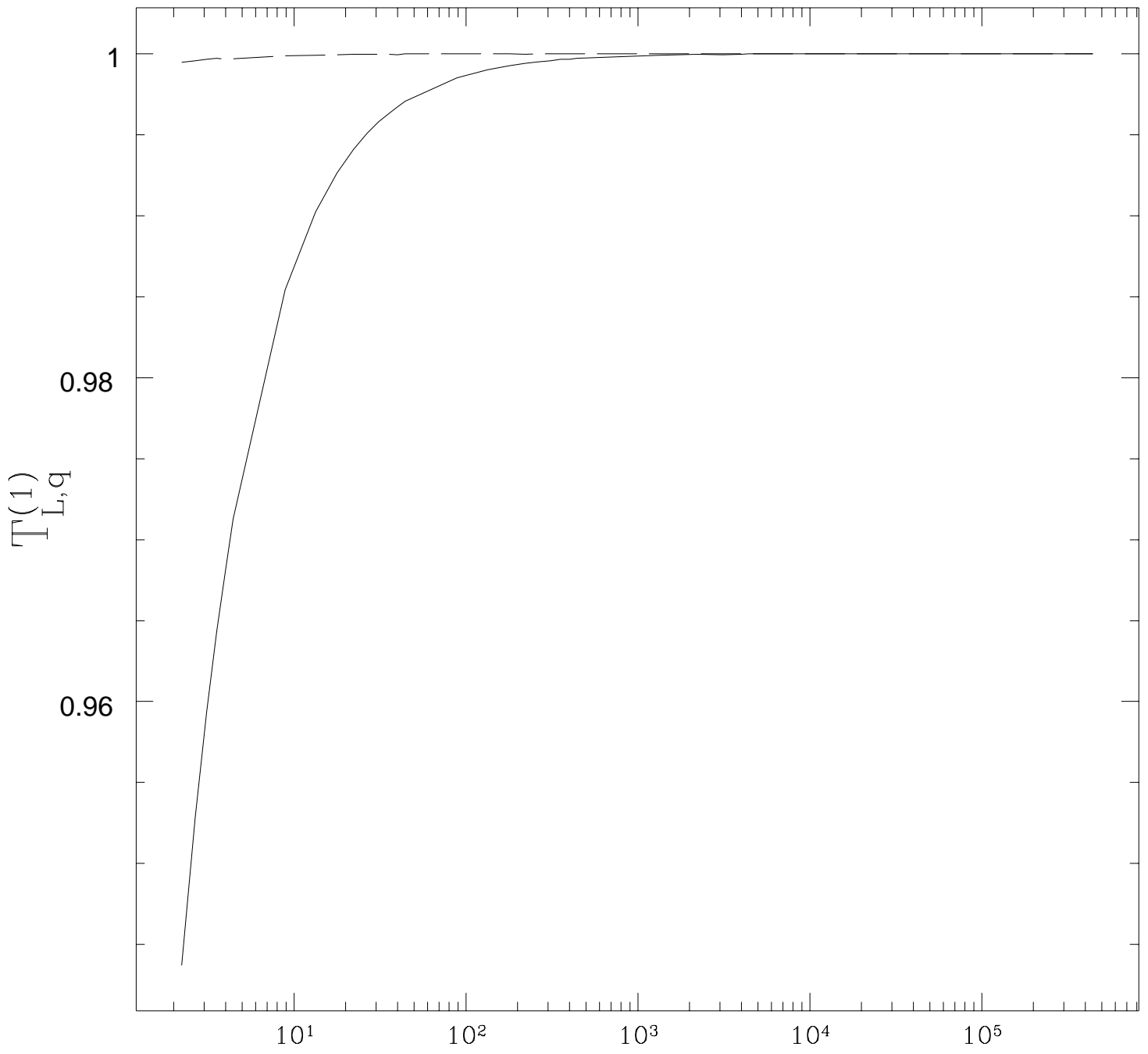


Fig. 9

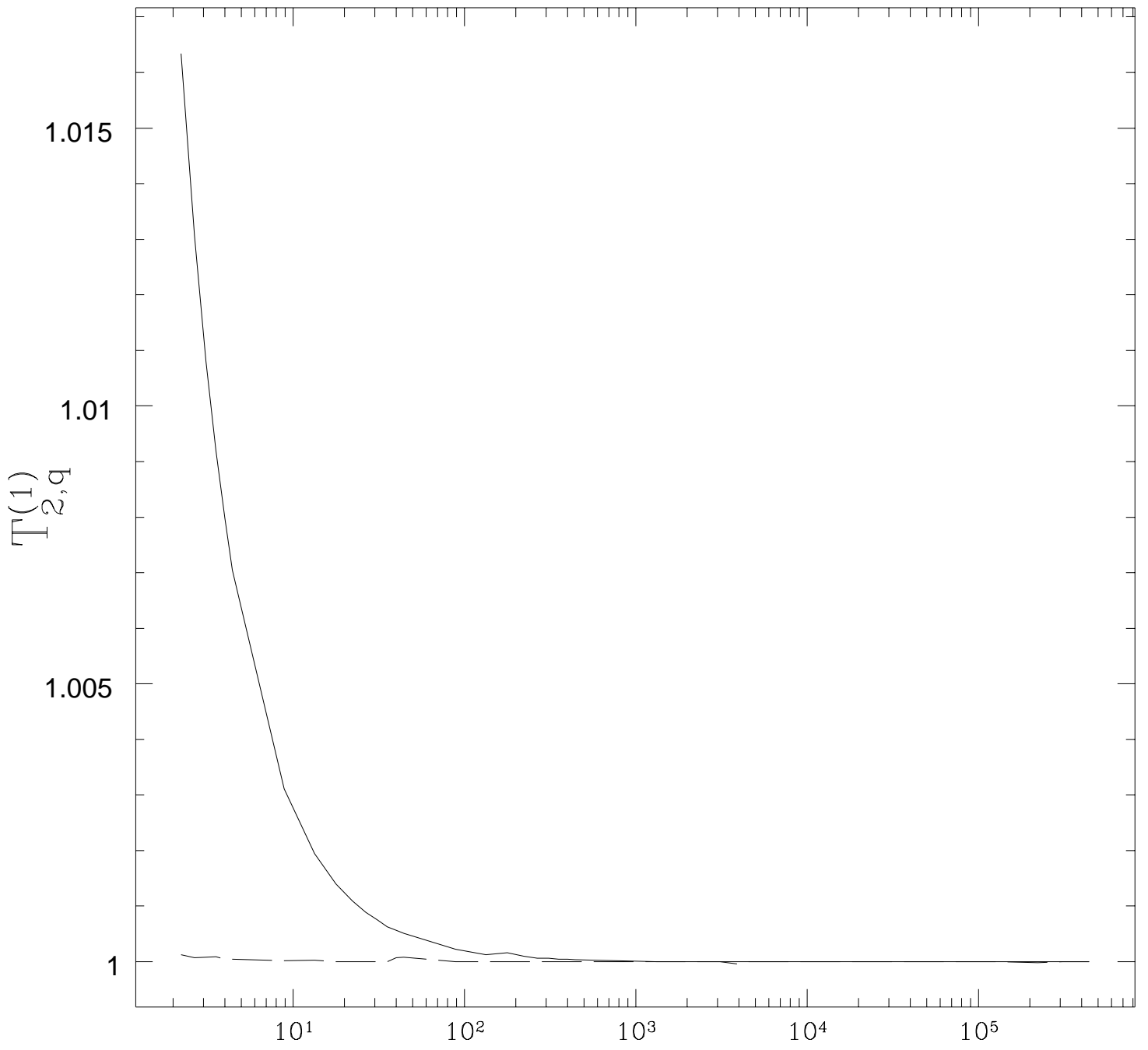


Fig. 10